# Expansions for infinite or finite plane circular time-reversal mirrors and acoustic curtains for wave-field-synthesis

Tim Mellow
*Mellow Acoustics Ltd., Farnham, Surrey GU9 9QH, United Kingdom*

Leo Kärkkäinen[a)]
*Nokia Research Center, 00180, Helsinki, Finland*

(Received 22 July 2013; revised 30 December 2013; accepted 21 January 2014)

An acoustic curtain is an array of microphones used for recording sound which is subsequently reproduced through an array of loudspeakers in which each loudspeaker reproduces the signal from its corresponding microphone. Here the sound originates from a point source on the axis of symmetry of the circular array. The Kirchhoff-Helmholtz integral for a plane circular curtain is solved analytically as fast-converging expansions, assuming an ideal continuous array, to speed up computations and provide insight. By reversing the time sequence of the recording (or reversing the direction of propagation of the incident wave so that the point source becomes an "ideal" point sink), the curtain becomes a time reversal mirror and the analytical solution for this is given simultaneously. In the case of an infinite planar array, it is demonstrated that either a monopole or dipole curtain will reproduce the diverging sound field of the point source on the far side. However, although the real part of the sound field of the infinite time-reversal mirror is reproduced, the imaginary part is an approximation due to the missing singularity. It is shown that the approximation may be improved by using the appropriate combination of monopole and dipole sources in the mirror.
© *2014 Acoustical Society of America*. [http://dx.doi.org/10.1121/1.4864459]

PACS number(s): 43.60.Tj, 43.20.Bi [HCS] Pages: 1256–1277

## I. INTRODUCTION

In this paper, we investigate two practical problems which may be evaluated using the Kirchhoff-Helmholtz boundary integral. The first is the "acoustic curtain"[1] in which a planar array of microphones is used during a recording and the output of each microphone is heard through a corresponding loudspeaker in an array during playback. This is known as "wave field synthesis."[2,3] In practice an array of microphones is usually made just large enough to make a reasonable approximation to an infinite array and the spacing between each is made small enough to avoid spatial aliasing. It should be noted that the sound field on the opposite side of the curtain from the sources is reproduced on both sides of the loudspeaker array if they are omnidirectional monopoles. The same also applies to dipoles except that the two sides have opposite phase.

Although it is not physically possible to reproduce the sound field on the same side of the acoustic curtain as the sources, this field may be calculated using a technique known as near-field acoustic holography.[4,5] The Green's function within the Kirchhoff-Helmholtz boundary integral is itself in integral form so that the resulting expression may be considered as a double Fourier transform. The first transform produces a spatial spectrum of the field within the array, which is propagated in the spatial frequency domain to the (parallel) observation plane where the second or inverse transform takes place.

The second problem to be studied is that of the time reversal mirror. Here the recording from the microphone array is played back through the loudspeaker array in reverse. However, if the recording is that of a simple periodic point source, we find that the wave from the loudspeaker array simply converges toward the position of the original source and then diverges again on the other side without reproducing the singularity of the original.[6] This is because the imaginary part of the pressure changes sign as the converging wave switches to a diverging one. It is therefore zero at the position of the original point source instead of infinity, although the finite real part is faithfully reproduced. In order to illustrate this, let us consider a diverging spherical wave such as that produced by a point source

$$\tilde{p}_d(r) = ik\rho c\tilde{U}_d \frac{e^{-ikr}}{4\pi r} = k\rho c\tilde{U}_d \frac{\sin kr + i\cos kr}{4\pi r}, \qquad (1)$$

where $r$ is the radial ordinate, $\tilde{U}_d$ is the volume velocity of the source at $r=0$, $k=\omega/c$ is the wave number, $\omega$ is the angular frequency, $c$ is the wave propagation speed, and $\rho$ is the density of the medium. Then the expression for a converging wave, such as that produced by an "ideal" point sink, is

$$\tilde{p}_c(r) = ik\rho c\tilde{U}_c \frac{e^{ikr}}{4\pi r} = k\rho c\tilde{U}_c \frac{-\sin kr + i\cos kr}{4\pi r}, \qquad (2)$$

where $\tilde{U}_c$ is the volume velocity at $r=0$. Notice that in both cases the real part of the pressure is finite at the origin $r=0$ whereas the imaginary part is singular. Imagine now that a converging spherical wave from a spherical time-reversal

[a)]Author to whom correspondence should be addressed. Electronic mail: leo.m.karkkainen@nokia.com

 0001-4966/2014/135(3)/1256/22/$30.00 © 2014 Acoustical Society of America

mirror passes through the origin and comes back out again as a diverging one (without any reflections from the inner surface of the mirror). There is neither a source nor a sink at the origin so that, for reasons of continuity, we now have $\tilde{U}_d = -\tilde{U}_c = \tilde{U}$ which yields

$$\tilde{p}_d(r) = ik\rho c\tilde{U}\frac{e^{-ikr}}{4\pi r} = k\rho c\tilde{U}\frac{\sin kr + i\cos kr}{4\pi r}, \tag{3}$$

$$\tilde{p}_c(r) = -ik\rho c\tilde{U}\frac{e^{ikr}}{4\pi r} = k\rho c\tilde{U}\frac{\sin kr - i\cos kr}{4\pi r}, \tag{4}$$

and a resultant time-reversal field of

$$\begin{aligned}\tilde{p}_{tr}(r) &= \tilde{p}_d(r) + \tilde{p}_c(r) = ik\rho c\tilde{U}\left(\frac{e^{ikr}}{4\pi r} - \frac{e^{-ikr}}{4\pi r}\right)\\ &= k\rho c\tilde{U}_d\frac{\sin kr}{2\pi r},\end{aligned} \tag{5}$$

which is continuous at $r = 0$. Hence the real parts of $\tilde{p}_d(r)$ and $\tilde{p}_c(r)$ have the same signs but signs of the imaginary parts are opposite. Also, the resultant pressure gradient at the origin $\partial\tilde{p}(r)/\partial r|_{r=0}$ is zero, so that as the converging waves pass through the origin and back out again as diverging ones, it is equivalent to their being reflected from a rigid termination at the origin.

It has been said that when time-reversing the waves produced by dropping a pebble in a pond, a pebble must rise out of the water at the end of the sequence[7] in order to truly replicate the original field. Hence one could place an active point sink at the location of the original source,[6] which is in effect a point source with reversed polarity. We see that combining such a source from Eq. (3) with the time-reversal field of Eq. (5) gives the ideal point sink field of Eq. (4). In other words, $\tilde{p}_c(r) = \tilde{p}_{tr}(r) - \tilde{p}_d(r)$.

Alternatively one could use a passive sink in the form of a sphere, which would need to have a surface impedance equal to that of free space and a diameter somewhat larger than the wavelength. This is described in greater detail in Appendix C.

Returning now to the problem of the planar time-reversal mirror, using a sink would require *a priori* knowledge of the original source position. To overcome this, Conti *et al.* propose "near-field time-reversal,"[8] which calculates the time-reversal field in a similar manner to near-field acoustic holography. Furthermore, Rosny and Fink demonstrate the advantage of using a purely dipole mirror in near-field time reversal in order to achieve sub-wavelength resolution.[9]

However, in this paper we show that a reasonable approximation (albeit limited by the classical half-wavelength diffraction limit) may be made outside the immediate vicinity of the source without using sinks or near-field techniques (Fourier transforms) in order to represent a practical physical situation. It is interesting to note that while the amplitude of the imaginary part of the pressure may be zero at the location of the original point source, it can become quite large on either side at high frequencies, albeit of opposite polarity, like a dipole. Hence it is possible to observe a "caustic" or "focusing" effect in the time-reversal field. Discretization effects are not considered here as the mirror is continuous, but this does give us the theoretical performance limit of a discretized system and most importantly yields analytical solutions to the Kirchhoff-Helmholtz boundary integral by means of suitable expansions. For instance, the expansion for the pressure-gradient (used in the monopole integral) draws on a previous result for a resilient disk in free space.[10] The fast converging expansions developed here are much more amenable to computation than evaluating the original integrals numerically (especially those for the infinite mirror and curtain) and have been used by the authors to generate computer animations for further insight.

Also, complicating factors such as room reflections are not considered as the purpose of this paper is to study the inherent limitations of the problem with relatively simple and easily computable expressions. Hence, the curtain and mirror are evaluated in free space, although a model of an infinite wall is included automatically in the monopole case through the boundary condition of zero velocity in the plane in which it is located.

The Kirchhoff-Helmholtz boundary integral is a mathematical expression of the Huygens-Fresnel principle, which states that if each point on a wave-front is replaced by a point source, the outward traveling wave will be reproduced.[11,12] The fact that this also produces an inward traveling wave need not matter if the surface on which the point sources are located fully envelopes the original source and we are only interested in the "external" field. This is also the case if the point sources cover an infinite plane because the opposite side of a plane to the original source is still fully isolated from it. In an infinite array, the sources may be monopoles in which case it is necessary to evaluate the velocity at each point. Alternatively, they may be dipoles in which case the pressure at each point must be evaluated.

If field strength at an arbitrary location $\mathbf{r}$ due to a point source at $\mathbf{r}_0$ is expressed by the Green's function $g(\mathbf{r}|\mathbf{r}_0)$ and the pressure at $\mathbf{r}_0$ is $p(\mathbf{r}_0)$, the Kirchhoff-Helmholtz boundary integral may be written as

$$\tilde{p}(\mathbf{r}) = \int\int g(\mathbf{r}|\mathbf{r}_0)\frac{\partial}{\partial n_0}\tilde{p}(\mathbf{r}_0) - \tilde{p}(\mathbf{r}_0)\frac{\partial}{\partial n_0}g(\mathbf{r}|\mathbf{r}_0)dS_0, \tag{6}$$

where the first term (or *monopole* part) is the integral of the product of the inward pointed normal gradient of the boundary values of $p(\mathbf{r}_0)$ and $g(\mathbf{r}|\mathbf{r}_0)$ over the surface and the second term (or *dipole* part) is the integral of the product of the boundary values of $p(\mathbf{r}_0)$ and the inward pointed normal gradient of $g(\mathbf{r}|\mathbf{r}_0)$ over the surface. In this form, we have a somewhat asymmetrical radiator because there will be a degree of cancellation (depending on the surface pressure and pressure-gradient values) between the monopole and dipole terms on one side of the surface, but in this paper we shall consider each term separately and how best to combine them.

In the case of a finite circular planar source, the Kirchhoff-Helmholtz integral is still valid over the surface of the source provided that the boundary conditions in the plane beyond its perimeter are met. That is, we would have zero normal pressure-gradient (or velocity) if it were a monopole or zero pressure if it were a dipole.

While the theory of the Kirchhoff-Helmholtz integral[11,12] predicts that it is sufficient to use *either* monopole pressure-gradient (velocity) sources *or* dipole pressure sources to create an infinite planar acoustic curtain, the choice of combination to give the best results in a time-reversal mirror is not predicted. However, in this investigation it is shown that a pure dipole time-reversal mirror yields best results between the plane of the source and the mirror, whereas a combination of a double-strength monopole and anti-phase dipole time-reversal mirror works best elsewhere. The mirror is created by reversing the direction of propagation of the incident wave from the original source, which is achieved by changing the signs in the exponents representing the pressure-gradient and pressure terms in the cases of the monopole and dipole integrals, respectively (i.e., changing $e^{-ikr}$ to $e^{ikr}$). The point source is a particularly useful example because it can form the basic building block of any source distribution.

Section II of this paper deals with finite and infinite curtains and mirrors using the monopole part of the Kirchhoff-Helmholtz integral while Sec. III deals with those using the dipole part. In both cases, Subsection A derives the fields in the plane of the curtain/mirror, which are the pressure-gradient in Sec. II and the pressure in Sec. III. Subsection B then presents expressions for the pressure field where the distance from the origin to the observation point is greater than the radius of the mirror/curtain ($r > a$). Subsection C presents those for where the distance from the origin to the observation point is less than the radius of the mirror/curtain ($r < a$). Full derivations are given in Appendix A. In order to avoid duplicating equations, it should be noted that the exponents in this paper can have either negative signs, representing diverging waves, or positive ones, representing converging waves. In such cases, the sign will be in the form $\mp$ where the upper sign represents the acoustic curtain solution and the lower sign represents the time-reversal mirror one. Similarly, the spherical Hankel function will appear in the form $h_n^{(2\backslash 1)}$, where the "2" denotes the acoustic curtain solution and the "1" represents the time-reversal mirror one. Some examples of calculated fields are presented using these solutions and discussed. In particular, the differences between the monopole and dipole time-reversed fields and the original point source are highlighted, with some suggestions for optimum combinations.

In all of the three-dimensional pressure-field plots, the circular curtain/mirror is located in the $xy$-plane with its center at the origin. Due to symmetry, the magnitudes of fields are the same on both sides of the $xy$-plane. Therefore, for convenience, they are plotted on the positive-$z$ side only in normalized axially-symmetric cylindrical coordinates $w/d$ and $z/d$, where the radial ordinate is $w = \sqrt{x^2 + y^2}$, and $d$ is the axial distance between the original point source and the origin. The normalized position of the original point source in the plots is at $w = 0$ and $z = 1$. In the equations, polar coordinates are also used where $w = r \sin\theta$ and $z = r \cos\theta$.

## II. FINITE PLANE CIRCULAR ACOUSTIC CURTAIN OR TIME-REVERSAL MIRROR USING MONOPOLE (PRESSURE-GRADIENT) SOURCE ARRAY

### A. Normal pressure-gradient or velocity in the *xy*-plane ($z = 0$) due to original point source

Before solving the monopole Kirchhoff-Helmholtz integral, we need to derive an expansion for the pressure-gradient in the plane of the curtain/mirror due to the original point source. This expansion will then be inserted into the monopole part of the Kirchhoff-Helmholtz integral. The point source shown in Fig. 1(a) produces the pressure field

$$\tilde{p}_S(w, \phi, z) = ik\rho c\tilde{U}_S g(w, \phi, z|r_0, \theta_0), \tag{7}$$

where $k = \omega/c$ is the wave number, $\rho$ is the density of air, $c$ is the wave propagation speed, and $\tilde{U}_S$ is the volume velocity of the source. The Green's function $g(w, \phi, z|r_0, \theta_0)$ is given in cylindrical-spherical coordinates by

$$g(w, \phi, z|r_0, \theta_0) = \frac{e^{\mp ikr_1}}{4\pi r_1}, \tag{8}$$

where $w$, $\phi$, and $z$ are the radial, azimuthal, and axial cylindrical ordinates, respectively, $r_0$ and $\theta_0$ are the radial and inclinational spherical coordinates, respectively, and $r_1$ is the distance from the source to the observation point where

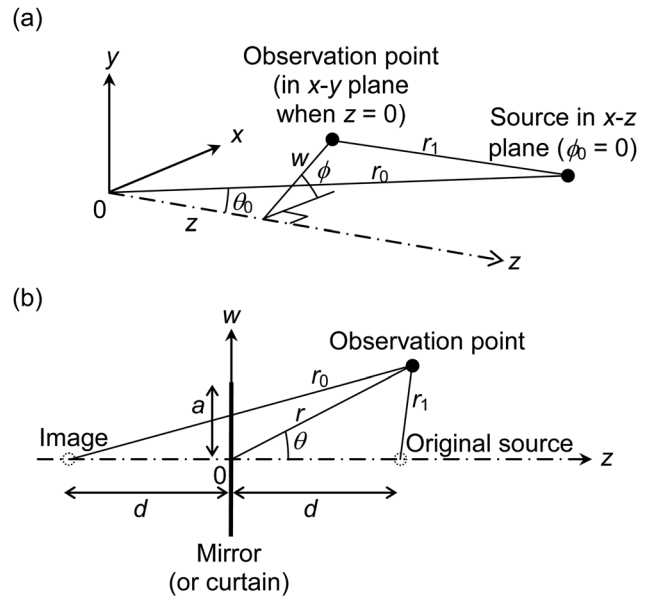


FIG. 1. Geometry of (a) field due to original point source and (b) field reproduced by time-reversal mirror or acoustic curtain. Although field reproduced by the latter originates from the negative-$z$ side of the curtain, the same field is reproduced on both sides of the $x$-$y$ plane so it is convenient to calculate it on the positive-$z$ side.

$$r_1^2 = r_0^2 + w^2 + z^2 - 2r_0(w\cos\phi\sin\theta_0 + z\cos\theta_0). \quad (9)$$

We eventually let $r_0 = d$ and $\theta_0 = 0$. Note that the sign of the exponent can be positive or negative. A negative sign denotes an outgoing wave (or source) and a positive sign denotes an incoming one (or sink). The normal pressure-gradient in the $z = 0$ plane is given by

$$\frac{\partial}{\partial z}\tilde{p}_S(w,\phi,z)|_{z=0} = ik\rho c\tilde{U}_S g'(w,\phi,z|r_0,\theta_0), \quad (10)$$

where $g'$ is the Green's function normal gradient. By reciprocity, this can be obtained from a result previously derived as follows[10]

$$g'(w,\phi|r_0,\theta_0) = \frac{\partial}{\partial z}g(w,\phi,z|r_0,\theta_0)|_{z=0} = -\frac{1}{w\cos\phi}\frac{\partial}{\partial\theta_0}g(w,\phi|r_0,\theta_0), \quad (11)$$

where

$$g(w,\phi|r_0,\theta_0) = \frac{e^{\mp ikr}}{4\pi r}, \quad (12)$$

and $r^2 = r_0^2 + w^2 - 2r_0 w\cos\phi\sin\theta_0$. The Green's function can then be expanded using Gegenbauer's addition theorem[13]

$$g(w,\phi|r_0,\theta_0) = \begin{cases} \frac{ik}{4\pi}\sum_{q=0}^{\infty}(2q+1)h_q^{(2\backslash 1)}(kr_0)j_q(kw)P_q(\cos\phi\sin\theta_0), & r_0 > w \\ \frac{ik}{4\pi}\sum_{q=0}^{\infty}(2q+1)j_q(kr_0)h_q^{(2\backslash 1)}(kw)P_q(\cos\phi\sin\theta_0), & w > r_0, \end{cases} \quad (13)$$

where $h_q^{(2)}$ is the spherical Hankel function for an outgoing wave defined by

$$h_p^{(2)}(kr) = j_p(kr) - iy_p(kr). \quad (14)$$

$h_q^{(1)}$ is the spherical Hankel function for an incoming wave defined by

$$h_p^{(1)}(kr) = j_p(kr) + iy_p(kr), \quad (15)$$

and $j_p$, $y_p$ are the spherical Bessel functions defined by

$$j_p(kr) = \sqrt{\frac{\pi}{2kr}}J_{p+1/2}(kr), \quad (16)$$

$$y_p(kr) = \sqrt{\frac{\pi}{2kr}}Y_{p+1/2}(kr). \quad (17)$$

After gathering Eqs. (10)–(13), differentiating with respect to $\theta_0$ and setting $\theta_0 = 0$ and $r_0 = d$, we have

$$\frac{\partial}{\partial z}\tilde{p}_S(w,z)|_{z=0} = -\frac{k^2\rho c\tilde{U}_S}{4\pi w}\sum_{q=0}^{\infty}(q+1) \times (2q+1)h_q^{(2\backslash 1)}(kd)j_q(kw)P_{q+1}(0). \quad (18)$$

However, only the odd terms are non-zero, so that

$$\frac{\partial}{\partial z}\tilde{p}_S(w,z)|_{z=0,w>d} = -\frac{k^2\rho c\tilde{U}_S}{2\pi w}\sum_{q=0}^{\infty}(q+1)(4q+3) \times h_{2q+1}^{(2\backslash 1)}(kd)j_{2q+1}(kw)P_{2q+2}(0), \quad (19)$$

$$\frac{\partial}{\partial z}\tilde{p}_S(w,z)|_{z=0,0\le w\le d} = -\frac{k^2\rho c\tilde{U}_S}{2\pi w}\sum_{q=0}^{\infty}(q+1) \times (4q+3)j_{2q+1}(kd) \times h_{2q+1}^{(2\backslash 1)}(kw)P_{2q+2}(0). \quad (20)$$

The particle velocity in the $z = 0$ plane is then given by

$$\tilde{u}_0(w) = \frac{1}{ik\rho c}\frac{\partial}{\partial z}\tilde{p}_S(w,z)|_{z=0}. \quad (21)$$

The point source will be replaced with a planar array of sources at $z = 0$ with this velocity distribution.

### B. Pressure field where the distance from the origin to the observation point is greater than the radius of the mirror or curtain ($r > a$)

We now replace the point source with a circular monopole array of radius $a$ in the $x$-$y$ plane with its center at the origin, as shown in Fig. 1(b), using the monopole Kirchhoff-Helmholtz boundary integral. Then the reconstructed pressure field $\tilde{p}_M(r,\theta)$ is given by integrating in $w_0$ and $\phi_0$ over the surface of the circular mirror/curtain

$$\tilde{p}_M(r,\theta) = -2\int_0^{2\pi}\int_0^a \frac{\partial}{\partial z_0}\tilde{p}_S(w_0,z_0)|_{z_0=0} \times g(r,\theta|w_0,\phi_0,z_0)|_{z_0=0}w_0 dw_0 d\phi_0, \quad (22)$$

where $g(r, \theta|w_0, \phi_0, z_0)$ is the Green's function in spherical-cylindrical coordinates defined by

$$g(r,\theta|w_0,\phi_0,z_0) = e^{-ikr_1}/(4\pi r_1), \quad (23)$$

where $r$ and $\theta$ are the radial and inclinational spherical coordinates, respectively, $w_0$, $\phi_0$, and $z_0$ are the radial, azimuthal, and axial cylindrical ordinates, respectively, and $r_1$ is the distance from the source to the observation point where

$$r_1^2 = r^2 + w_0^2 + z_0^2 - 2r(w_0\cos\phi_0\sin\theta + z_0\cos\theta). \quad (24)$$

In Appendix A, Eq. (22) is solved to give the following solutions:

If $a < d$, then the outer solution ($r > a$) is given by

$$\tilde{p}_M(r,\theta)|_{r>a,d>a} = \mp i\frac{k^2\rho c\tilde{U}_S}{4\pi^2}\sum_{p=0}^{P}\sum_{q=0}^{Q}(-1)^{p+q}g_{p,q}^{(M)}h_{2p}^{(2)}(kr) \times h_{2q+1}^{(2\backslash 1)}(kd)f_{p,q}^{(M1)}(ka)P_{2p}(\cos\theta), \quad (25)$$

where $g_{p,q}^{(M)}$ and $f_{p,q}^{(M1)}(ka)$ are given by Eqs. (A10) and (A11), respectively.

If $a \geq d$, then the outer solution ($r > a$) is given by

$$\tilde{p}_M(r,\theta)|_{r>a,0\leq d\leq a} = i\frac{k\rho c\tilde{U}_S}{8\pi}\left\{\left(\frac{e^{-ikr_0}}{r_0}+\frac{e^{-ikr_1}}{r_1}\right)\mp\frac{2k}{\pi}\sum_{p=0}^{P}\sum_{q=0}^{Q}(-1)^{p+q}\times g_{p,q}^{(M)}h_{2p}^{(2)}(kr)j_{2q+1}(kd)f_{p,q}^{(M2)}(ka)P_{2p}(\cos\theta)\right\}, \quad (26)$$

where $f_{p,q}^{(M2)}(ka)$ is given by Eq. (A15), $r_0^2 = r^2 + d^2 + 2rd|\cos\theta|$ and $r_1^2 = r^2 + d^2 - 2rd|\cos\theta|$.

### C. Pressure field where the distance from the origin to the observation point is less than the radius of the mirror or curtain ($r < a$)

If $a < d$, then the inner solution ($0 \leq r \leq a$) is given by

$$\tilde{p}_M(r,\theta)|_{0\leq r\leq a,d>a} = i\frac{k\rho c\tilde{U}_S}{8\pi}\left\{\left(\frac{e^{\mp ikr_0}}{r_0}-\frac{e^{\mp ikr_1}}{r_1}\right)\mp\frac{2k}{\pi}\sum_{p=0}^{P}\sum_{q=0}^{Q}(-1)^{p+q}\times g_{p,q}^{(M)}j_{2p}(kr)h_{2q+1}^{(2\backslash 1)}(kd)f_{p,q}^{(M3)}(ka)P_{2p}(\cos\theta)\right\}, \quad (27)$$

where $g_{p,q}^{(M)}$ and $f_{p,q}^{(M3)}(ka)$ are given by Eqs. (A10) and (A24), respectively.

If $a \geq d$, then the inner solution ($0 \leq r \leq a$) is given by

$$\tilde{p}_M(r,\theta)|_{0\leq r\leq a,0\leq d\leq a} = i\frac{k\rho c\tilde{U}_S}{8\pi}\left\{\frac{e^{-ikr_0}+e^{\mp ikr_0}}{r_0}+\frac{e^{-ikr_1}-e^{\mp ikr_1}}{r_1}\mp\frac{2k}{\pi}\sum_{p=0}^{P}\sum_{q=0}^{Q}(-1)^{p+q}g_{p,q}^{(M)}j_{2p}(kr)j_{2q+1}(kd)f_{p,q}^{(M4)}(ka)P_{2p}(\cos\theta)\right\}, \quad (28)$$

where $f_{p,q}^{(M4)}(ka)$ is given by Eq. (A34), $r_0^2 = r^2 + d^2 + 2rd|\cos\theta|$ and $r_1^2 = r^2 + d^2 - 2rd|\cos\theta|$.

## III. INFINITE PLANAR ACOUSTIC CURTAIN OR TIME-REVERSAL MIRROR USING MONOPOLE (PRESSURE-GRADIENT) SOURCE ARRAY

If $a = \infty$, then $f_{p,q}^{(M4)}(ka)|_{a\to\infty} = 2(-1)^{p+q}$ in the time-reversal mirror solution and $f_{p,q}^{(M4)}(ka)|_{a\to\infty} = 0$ in the acoustic curtain solution. Hence Eq. (28) reduces to

$$\tilde{p}_M(r,\theta)|_{a=\infty} = i\frac{k\rho c\tilde{U}_S}{4\pi} \times \begin{cases} \left(\frac{e^{-ikr_0}+e^{ikr_0}}{2r_0}+\frac{e^{-ikr_1}-e^{ikr_1}}{2r_1}+\frac{2k}{\pi}\sum_{p=0}^{P}\sum_{q=0}^{Q}g_{p,q}^{(M)}j_{2p}(kr)j_{2q+1}(kd)P_{2p}(\cos\theta)\right), & \text{time-reversal mirror} \\ \frac{e^{-ikr_0}}{r_0}, & \text{acoustic curtain.} \end{cases} \quad (29)$$

## IV. FINITE PLANE CIRCULAR ACOUSTIC CURTAIN OR TIME-REVERSAL MIRROR USING DIPOLE (PRESSURE) SOURCE ARRAY

### A. Pressure field in plane of curtain or mirror due to original point source

Before solving the dipole Kirchhoff-Helmholtz integral, we need to derive an expansion for the pressure in the plane of the curtain/mirror due to the original point source. This expansion will then be inserted into the dipole part of the Kirchhoff-Helmholtz integral. The point source shown in Fig. 1(a) produces the pressure field given by Eq. (7). If we set $r_0 = d$ and $\theta_0 = 0$ in Eq. (13), before inserting it in Eq. (7) and note that only the even terms are non-zero [using the identities of Eqs. (A5) and (A6)], we can write the following expansions for the pressure field due to the point source:

$$\tilde{p}_S(w,0)|_{d>w} = -\frac{k^2\rho c\tilde{U}_S}{4\pi^{3/2}}\sum_{q=0}^{\infty}\frac{(-1)^p(4q+1)\Gamma(p+1/2)}{p!}h_{2q}^{(2\backslash 1)}(kd)j_{2q}(kw), \tag{30}$$

$$\tilde{p}_S(w,0)|_{w>d} = -\frac{k^2\rho c\tilde{U}_S}{4\pi^{3/2}}\sum_{q=0}^{\infty}\frac{(-1)^p(4q+1)\Gamma(p+1/2)}{p!}j_{2q}(kd)h_{2q}^{(2\backslash 1)}(kw). \tag{31}$$

### B. Pressure field where the distance from the origin to the observation point is greater than the radius of the mirror or curtain

We now replace the point source with a circular dipole array of radius $a$ in the $x$-$y$ plane with its center at the origin, as shown in Fig. 1(b), using the dipole Kirchhoff-Helmholtz boundary integral. Then the reconstructed pressure field $\tilde{p}_D(r,\theta)$ is given by integrating in $w_0$ and $\phi_0$ over the surface of the circular mirror/curtain

$$\tilde{p}_D(r,\theta) = 2\int_{-\pi}^{\pi}\int_0^a \tilde{p}_S(w_0,0)\frac{\partial}{\partial z_0}g(r,\theta|w_0,\phi_0,z_0)|_{z=0+}w_0 dw_0 d\phi_0, \tag{32}$$

where $g(r,\theta|w_0,\phi_0,z_0)$ is the Green's function in cylindrical-spherical coordinates defined by

$$g(r,\theta|w_0,\phi_0,z_0) = e^{-ikr_1}/(4\pi r_1), \tag{33}$$

where

$$r_1^2 = r^2 + w_0^2 + z_0^2 - 2r(w_0\cos\phi_0\sin\theta + z_0\cos\theta). \tag{34}$$

In Appendix A, Eq. (32) is solved to give the following solutions:

If $a < d$, then the outer solution ($r > a$) is given by

$$\tilde{p}_D(r,\theta)|_{r>a,d>a} = -i\frac{k^2\rho c\tilde{U}_S}{8\pi^2}\sum_{p=0}^{P}\sum_{q=0}^{Q}(-1)^{p+q}g_{p,q}^{(D)}h_{2p+1}^{(2)}(kr)\times h_{2q}^{(2\backslash 1)}(kd)f_{p,q}^{(D1)}(ka)P_{2p+1}(\cos\theta), \tag{35}$$

where $g_{p,q}^{(D)}$ and $f_{p,q}^{(D1)}(ka)$ are given by Eqs. (A42) and (A43), respectively.

If $a \geq d$, then the outer solution ($r > a$) is given by

$$\tilde{p}_D(r,\theta)|_{r>a,0\leq d\leq a} = i\frac{k\rho c\tilde{U}_S}{8\pi}\left\{\pm\mathrm{sgn}(\cos\theta)\left(\frac{e^{-ikr_0}}{r_0}-\frac{e^{-ikr_1}}{r_1}\right) - \frac{2k}{\pi}\sum_{p=0}^{P}\sum_{q=0}^{Q}(-1)^{p+q}\right.$$
$$\left.\times g_{p,q}^{(D)}h_{2p+1}^{(2)}(kr)j_{2q}(kd)f_{p,q}^{(D2)}(ka)P_{2p+1}(\cos\theta)\right\}, \tag{36}$$

where $f_{p,q}^{(D2)}(ka)$ is given by Eq. (A46), $r_0^2 = r^2 + d^2 + 2rd|\cos\theta|$ and $r_1^2 = r^2 + d^2 - 2rd|\cos\theta|$.

### C. Pressure field where the distance from the origin to the observation point is less than the radius of the mirror or curtain

If $a < d$, then the inner solution ($0 \le r \le a$) is given by

$$\tilde{p}_D(r,\theta)|_{0\le r\le a, d>a} = i\frac{k\rho c\tilde{U}_S}{8\pi}\left\{\pm\mathrm{sgn}(\cos\theta)\left(\frac{e^{\mp ikr_0}}{r_0}+\frac{e^{\mp ikr_1}}{r_1}\right)-\frac{2k}{\pi}\sum_{p=0}^{P}\sum_{q=0}^{Q}(-1)^{p+q}\right.$$
$$\left.\times\, g_{p,q}^{(D)} j_{2p+1}(kr)h_{2q}^{(2\backslash 1)}(kd)f_{p,q}^{(D3)}(ka)P_{2p+1}(\cos\theta)\right\}, \tag{37}$$

where $g_{p,q}^{(D)}$ and $f_{p,q}^{(D3)}(ka)$ are given by Eqs. (A42) and (A54), respectively.

If $a \ge d$, then the inner solution ($0 \le r \le a$) is given by

$$\tilde{p}_D(r,\theta)|_{0\le r\le a, 0\le d\le a} = i\frac{k\rho c\tilde{U}_S}{8\pi}\left\{\pm\mathrm{sgn}(\cos\theta)\left(\frac{e^{-ikr_0}+e^{\mp ikr_0}}{r_0}-\frac{e^{-ikr_1}-e^{\mp ikr_1}}{r_1}\right)\right.$$
$$\left.-\frac{2k}{\pi}\sum_{p=0}^{P}\sum_{q=0}^{Q}(-1)^{p+q}g_{p,q}j_{2p+1}(kr)j_{2q}(kd)f_{p,q}^{(D4)}(ka)P_{2p+1}(\cos\theta)\right\}, \tag{38}$$

where $f_{p,q}^{(D4)}(ka)$ is given by Eq. (A64), $r_0^2 = r^2+d^2+2rd|\cos\theta|$ and $r_1^2 = r^2+d^2-2rd|\cos\theta|$.

## V. INFINITE PLANAR ACOUSTIC CURTAIN OR TIME-REVERSAL MIRROR USING DIPOLE (PRESSURE) SOURCE ARRAY

If $a=\infty$, then $f_{p,q}^{(D4)}(ka)|_{a\to\infty} = 2(-1)^{p+q}$ in the time-reversal mirror solution and $f_{p,q}^{(D4)}(ka)|_{a\to\infty} = 0$ in the acoustic curtain solution. Hence Eq. (38) reduces to

$$\tilde{p}_D(r,\theta)|_{a=\infty} = i\frac{k\rho c\tilde{U}_S}{4\pi}$$
$$\times\begin{cases}\left\{-\mathrm{sgn}(\cos\theta)\left(\dfrac{e^{-ikr_0}+e^{ikr_0}}{2r_0}-\dfrac{e^{-ikr_1}-e^{ikr_1}}{2r_1}\right)\right. & \\ \left.-\dfrac{2k}{\pi}\displaystyle\sum_{p=0}^{P}\sum_{q=0}^{Q}g_{p,q}^{(D)}j_{2p+1}(kr)j_{2q}(kd)P_{2p+1}(\cos\theta)\right\}, & \text{time-reversal mirror}\\ \mathrm{sgn}(\cos\theta)\dfrac{e^{-ikr_0}}{r_0}, & \text{acoustic curtain.}\end{cases} \tag{39}$$

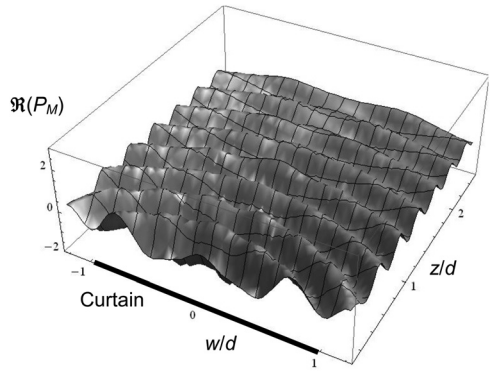


FIG. 2. Real part of reconstructed pressure field of *finite monopole* acoustic curtain at $kd=20$, where $a=d$ and $P_M = 4\pi d\tilde{p}_M/(k\rho c\tilde{U}_S)$ from Eq. (28). Plot is in cylindrical coordinates ($w$,$z$), where $w = r\sin\theta$ and $z = r\cos\theta$ and with the expansion limits set to $P=Q=4ka=4kd$.

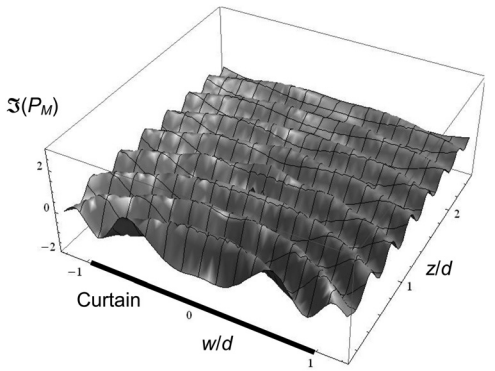


FIG. 3. Imaginary part of reconstructed pressure field of *finite monopole* acoustic curtain at $kd=20$, where $a=d$ and $P_M = 4\pi d\tilde{p}_M/(k\rho c\tilde{U}_S)$ from Eq. (28). Plot is in cylindrical coordinates ($w$,$z$), where $w = r\sin\theta$ and $z = r\cos\theta$ and with the expansion limits set to $P=Q=4ka=4kd$.

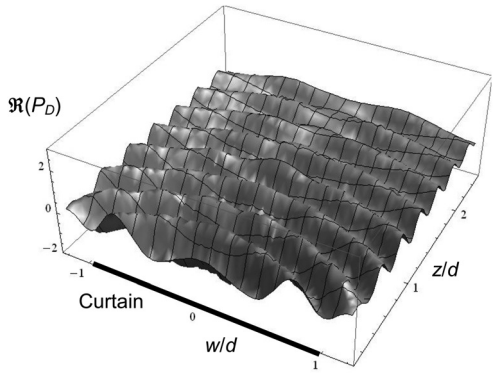


FIG. 4. Real part of reconstructed pressure field of *finite dipole* acoustic curtain at $kd = 20$, where $a = d$ and $P_D = 4\pi d\tilde{p}_D/(k\rho c\tilde{U}_S)$ from Eq. (38). Plot is in cylindrical coordinates $(w,z)$ where $w = r\sin\theta$ and $z = r\cos\theta$ and with the expansion limits set to $P = Q = 4ka = 4kd$.

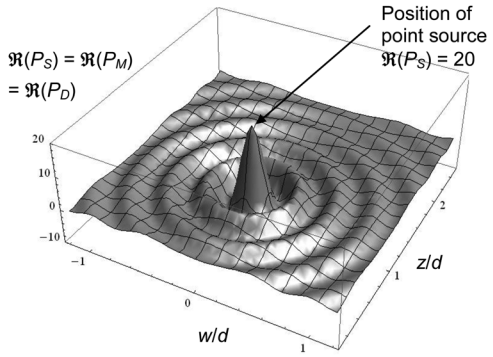


FIG. 6. Real part of pressure field of *original point source* (or real part of reconstructed pressure field of *infinite monopole* or *dipole* time-reversal mirror) at $kd = 20$, where $P_S = 4\pi d\tilde{p}_S/(k\rho c\tilde{U}_S)$ from Eq. (7), $P_M = 4\pi d\tilde{p}_M/(k\rho c\tilde{U}_S)$ from Eq. (29), and $P_D = 4\pi d\tilde{p}_D/(k\rho c\tilde{U}_S)$ from Eq. (39). Plot is in cylindrical coordinates $(w,z)$ where $w = r\sin\theta$ and $z = r\cos\theta$. Also, $r_0 = d$ and $\theta_0 = 0$.

## VI. DISCUSSION

### A. Acoustic curtain

Not surprisingly, the solutions given in Eqs. (29) and (39), for infinite monopole and dipole acoustic curtains, respectively, are simply the same as that for a point source on the negative-$z$ side of the plane when observed on the positive side, although the field is symmetrical either side of the $xy$-plane (except that the polarity is reversed in the case of the planar dipole source).

Interestingly, Eqs. (28) and (38) for the finite circular monopole and dipole planes, respectively, both have three terms. The first and second terms relate to point sources on the negative and positive-$z$ sides of the $xy$-plane, respectively. However, when we evaluate the field on the positive-$z$ side of an acoustic curtain, we find that their combination eliminates the point source on the positive side of the $xy$-plane leaving just the one on the negative side. However, the waves from that source can only be "seen" on the positive side because as soon as we evaluate the field on the negative side they appear to radiate from a source on the positive side onto the negative side. In other words, we have symmetry in the case of a monopole curtain or anti-symmetry in the case of a dipole one. The third term, or "diffraction" term, has a complicated far-field directivity pattern at $kd = 20$ with 60 side lobes between 0° and 90° off axis, none of which peak at more than 23 dB below the central lobe or "Airy disk." The −6 dB width of the central lobe is just ±0.7°.

The real and imaginary fields due to a *finite* monopole acoustic curtain are shown in Figs. 2 and 3, respectively, while the real and imaginary fields for a finite dipole one are shown in Figs. 4 and 5, respectively. Admittedly, the reconstructed fields are not optimum because the infinite plane has been simply truncated at $a = d$. Hence, there are discontinuities in the velocity (monopole) or pressure (dipole) boundary conditions equivalent to a rectangular window function and a better solution would be to include an apodization function.[14] However, these plots give some indication of what might be produced by a practical setup.

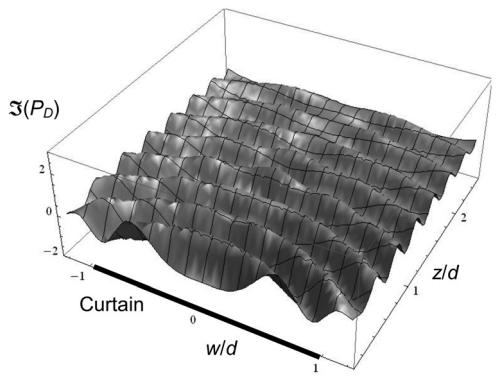


FIG. 5. Imaginary part of reconstructed pressure field of *finite dipole* acoustic curtain at $kd = 20$, where $a = d$ and $P_D = 4\pi d\tilde{p}_D/(k\rho c\tilde{U}_S)$ from Eq. (38). Plot is in cylindrical coordinates $(w,z)$ where $w = r\sin\theta$ and $z = r\cos\theta$ and with the expansion limits set to $P = Q = 4ka = 4kd$.

### B. Time-reversal mirror

The time reversed solution for the infinite plane is a little more complicated because the first two terms of Eqs. (28) and (38) represent the imaginary part of the field of a point

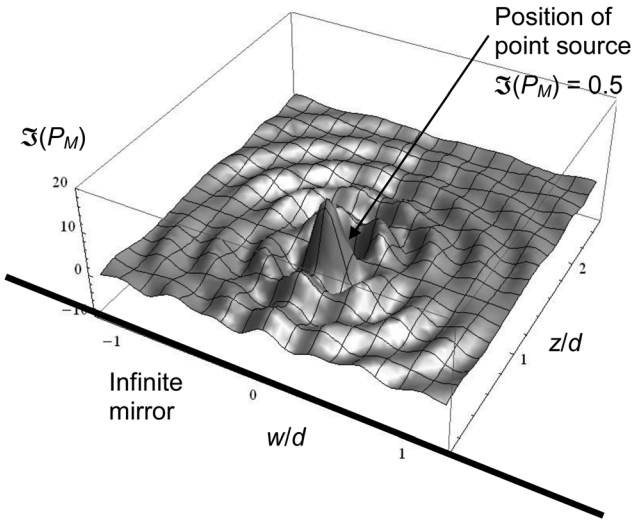


FIG. 7. Imaginary part of reconstructed pressure field of *infinite monopole* time-reversal mirror at $kd = 20$, where $P_M = 4\pi d\tilde{p}_M/(k\rho c\tilde{U}_S)$ from Eq. (29). Plot is in cylindrical coordinates $(w,z)$ where $w = r\sin\theta$ and $z = r\cos\theta$ and with the expansion limits set to $P = Q = 4ka = 4kd$. See Fig. 6 for real part.

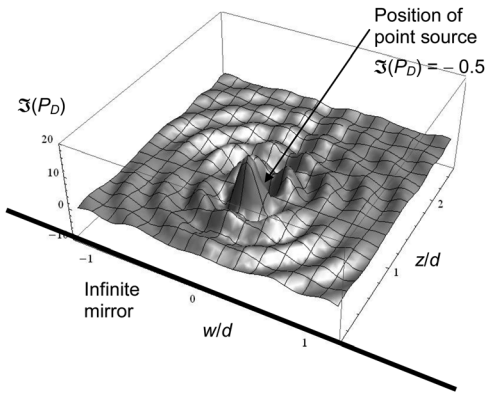


FIG. 8. Imaginary part of reconstructed pressure field of *infinite dipole* time-reversal mirror at $kd = 20$, where $P_D = 4\pi d\tilde{p}_D/(k\rho c\tilde{U}_S)$ from Eq. (39). Plot is in cylindrical coordinates $(w,z)$ where $w = r\sin\theta$ and $z = r\cos\theta$ and with the expansion limits set to $P = Q = 4ka = 4kd$. See Fig. 6 for real part.

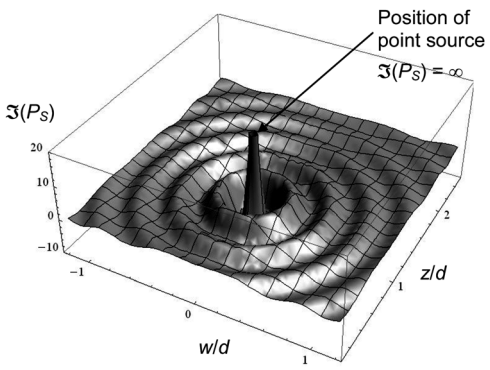


FIG. 9. Imaginary part of pressure field of *original point source* at $kd = 20$, where $P_S = 4\pi d\tilde{p}_S/(k\rho c\tilde{U}_S)$ from Eq. (7). Plot is in cylindrical coordinates $(w,z)$ where $w = r\sin\theta$ and $z = r\cos\theta$. Also, $r_0 = d$ and $\theta_0 = 0$.

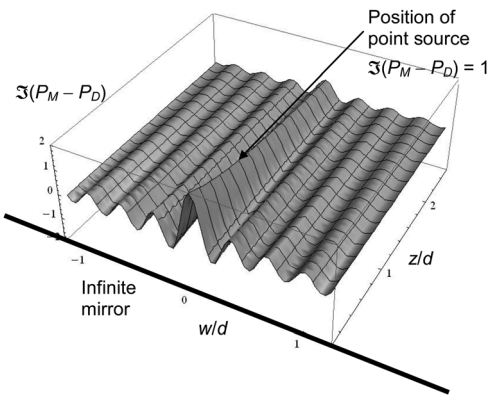


FIG. 10. Error function due to the difference between the imaginary monopole and dipole pressure fields of Figs. 7 and 8, where $P_M = 4\pi d\tilde{p}_M/(k\rho c\tilde{U}_S)$ and $P_D = 4\pi d\tilde{p}_D/(k\rho c\tilde{U}_S)$. Plot is in cylindrical coordinates $(w,z)$ where $w = r\sin\theta$ and $z = r\cos\theta$ and with the expansion limits set to $P = Q = 4ka = 4kd$.

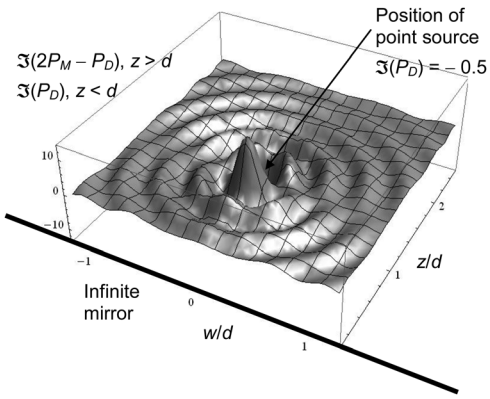


FIG. 11. Combined imaginary part of reconstructed pressure field of *infinite* time-reversal mirror as follows: For $z/d > 1$, plot shows double-strength monopole field less single-strength dipole field. For $z/d < 1$, plot shows single-strength dipole field only, where $P_M = 4\pi d\tilde{p}_M/(k\rho c\tilde{U}_S)$ and $P_D = 4\pi d\tilde{p}_D/(k\rho c\tilde{U}_S)$. Plot is in cylindrical coordinates $(w,z)$, where $w = r\sin\theta$ and $z = r\cos\theta$ and with the expansion limits set to $P = Q = 4ka = 4kd$.

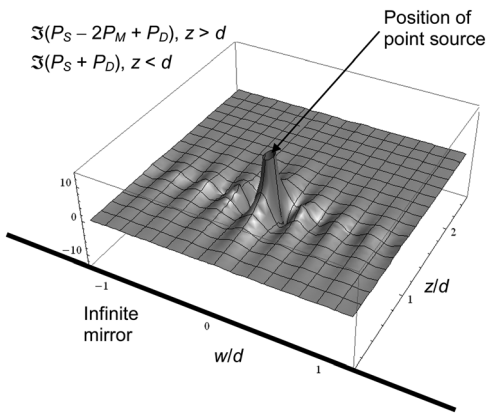


FIG. 12. Difference between imaginary reconstructed pressure fields shown in Fig. 9 and Fig. 11, where $P_S = 4\pi d\tilde{p}_S/(k\rho c\tilde{U}_S)$, $P_M = 4\pi d\tilde{p}_M/(k\rho c\tilde{U}_S)$, and $P_D = 4\pi d\tilde{p}_D/(k\rho c\tilde{U}_S)$. Plot is in cylindrical coordinates $(w,z)$, where $w = r\sin\theta$ and $z = r\cos\theta$ and with the expansion limits set to $P = Q = 4ka = 4kd$.

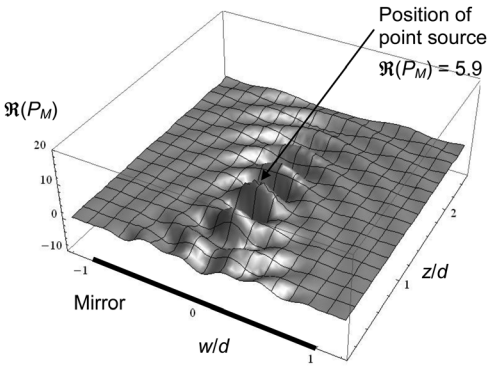


FIG. 13. Real part of reconstructed pressure field of *finite monopole* time-reversal mirror at $kd = 20$, where $a = d$ and $P_M = 4\pi d\tilde{p}_M/(k\rho c\tilde{U}_S)$ from Eq. (28). Plot is in cylindrical coordinates $(w,z)$, where $w = r\sin\theta$ and $z = r\cos\theta$ and with the expansion limits set to $P = Q = 4ka = 4kd$.

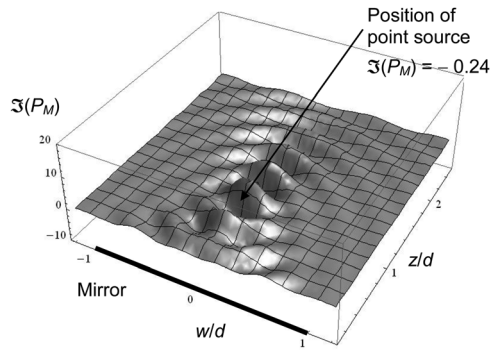


FIG. 14. Imaginary part of reconstructed pressure field of *finite monopole* time-reversal mirror at $kd = 20$, where $a = d$ and $P_M = 4\pi d\tilde{p}_M/(k\rho c\tilde{U}_S)$ from Eq. (28). Plot is in cylindrical coordinates $(w,z)$, where $w = r\sin\theta$ and $z = r\cos\theta$ and with the expansion limits set to $P = Q = 4ka = 4kd$.

source on the negative-$z$ side and the real part (see Fig. 6) on the positive-$z$ side, respectively. Also, the third term does not vanish as the radius approached infinity but simplifies as shown in Eqs. (29) and (39), and thus provides an additional imaginary term. However, the monopole and dipole time-reversed imaginary pressure fields shown in Figs. 7 and 8, respectively, differ somewhat from that of the simple point source shown in Fig. 9. To begin with, the singularity at the center of the original point source is absent. This is due to the fact that the waves from the planar source travel *into* the focal point and then *out* again the other side. Hence, the phase changes in the plane of the focal point where the imaginary pressure is positive on one side and negative on the other. Therefore it is substantially canceled in the plane of the focal point where the positive and negative imaginary pressures meet, as can be seen in Figs. 7 and 8. Another noticeable difference is that these time-reversed imaginary pressure fields have ripples, due to interference patterns, which are absent in the original point source. When taking the difference between them, as shown in Fig. 10, an error function becomes apparent, which is given by

$$\Im(\tilde{p}_M - \tilde{p}_D) = \tilde{p}_E = k\rho c\tilde{U}_S \frac{J_0(kw)}{2\pi(z+d)}. \tag{40}$$

Hence it represents an incoming cylindrical wave which passes through the $z$ axis and travels back out again. It also

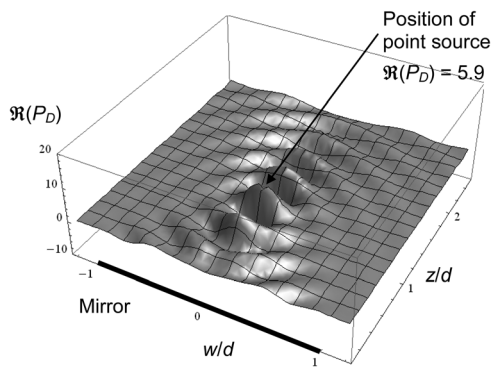


FIG. 15. Real part of reconstructed pressure field of *finite dipole* time-reversal mirror at $kd = 20$, where $a = d$ and $P_D = 4\pi d\tilde{p}_D/(k\rho c\tilde{U}_S)$ from Eq. (38). Plot is in cylindrical coordinates $(w,z)$ where $w = r\sin\theta$ and $z = r\cos\theta$ and with the expansion limits set to $P = Q = 4ka = 4kd$.

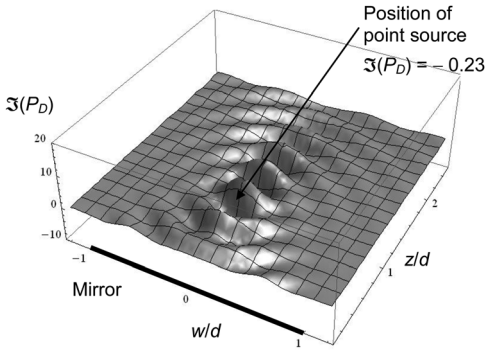


FIG. 16. Imaginary part of reconstructed pressure field of *finite dipole* time-reversal mirror at $kd = 20$, where $a = d$ and $P_D = 4\pi d\tilde{p}_D/(k\rho c\tilde{U}_S)$ from Eq. (38). Plot is in cylindrical coordinates $(w,z)$ where $w = r\sin\theta$ and $z = r\cos\theta$ and with the expansion limits set to $P = Q = 4ka = 4kd$.

decays with increasing $z$. This error is distributed unequally between the monopole and dipole fields as follows:

$$\Im(\tilde{p}_S) \approx \begin{cases} \Im(\tilde{p}_M) + \tilde{p}_E, & z > d \\ -\Im(\tilde{p}_M) + \tilde{p}_E, & z < d, \end{cases} \tag{41}$$

$$\Im(\tilde{p}_S) \approx \begin{cases} \Im(\tilde{p}_D) + 2\tilde{p}_E, & z > d \\ -\Im(\tilde{p}_D), & z < d, \end{cases} \tag{42}$$

except at $(z, w) = (d, 0)$ or in the immediate vicinity, due to the loss of the singularity. It is perhaps not surprising that the dipole field in the vicinity of the plane has the least error because the dipole Kirchhoff-Helmholtz integral actually contains the pressure distribution of the original point source within the plane. Therefore, the error in the plane should be zero. The imaginary pressure field of the original point source can be approximated using the following combination of monopole and dipole planar sources:

$$\Im(\tilde{p}_S) \approx \begin{cases} \Im(2\tilde{p}_M - \tilde{p}_D), & z > d \\ \Im(-\tilde{p}_D), & z < d \end{cases} \tag{43}$$

as shown in Fig. 11, where the interference patterns have largely disappeared. Unfortunately one cannot have simultaneously a good reconstruction of $\Im(\tilde{p}_S)$ for $z > d$ and $z < d$

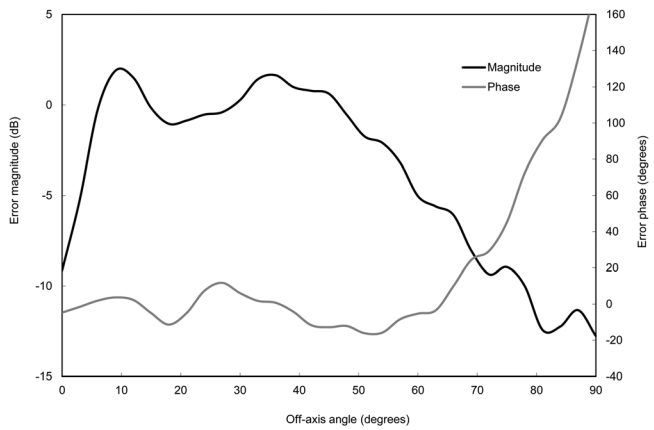


FIG. 17. Error magnitude and phase between reconstructed pressure field of *finite monopole* time-reversal mirror and original point source versus angle off-axis $\theta_1$ at a distance of $r_1 = 2d$ from the position of the source, where $a = 2d$, $r_0^2 = r_1^2 + 4d^2 + 4r_1 d\cos\theta_1$, $r^2 = r_1^2 + d^2 + 2r_1 d\cos\theta_1$, and $\cos\theta = (r^2 + d^2 - r_1^2)/(2rd)$. Plot of $20\log_{10}(|P_M/P_S|)$. As would be expected from a point source, $P_S$ is independent of $\theta_1$.

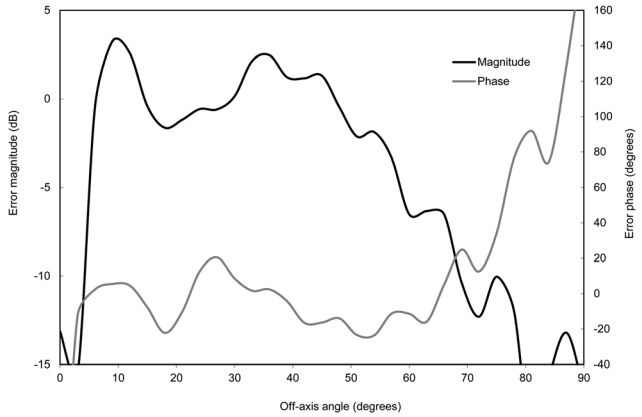


FIG. 18. Error magnitude and phase between reconstructed pressure field of *finite dipole* time-reversal mirror and original point source versus off-axis angle $\theta_1$ at a distance of $r_1 = 2d$ from the position of the source, where $a = 2d$, $r_0{}^2 = r_1{}^2 + 4d^2 + 4r_1 d\cos\theta_1$, $r^2 = r_1{}^2 + d^2 + 2r_1 d\cos\theta_1$, and $\cos\theta = (r^2 + d^2 - r_1{}^2)/(2rd)$. Plot of $20\log_{10}(|P_M/P_S|)$. As would be expected from a point source, $P_S$ is independent $\theta_1$.

because the field superpositions are different. Again, this breaks down at $z = d$ and $w = 0$, and in the immediate vicinity, due to the loss of the singularity. The difference between the imaginary pressure field of Fig. 11 and the original point source is shown in Fig. 12. Apart from the missing singularity at the center, there are also errors in the plane of the point source and either side of it due to the phase reversal. Otherwise, the reconstruction appears to be fairly accurate. Furthermore, the above relationships appear to hold at any frequency.

The real and imaginary fields due to a *finite* monopole time reversal mirror are shown in Figs. 13 and 14, respectively, while the real and imaginary fields for a finite dipole one are shown in Figs. 15 and 16, respectively. The same comments made above, with respect to the acoustic curtain, about the lack of a smooth windowing function apply here also. For illustration, the errors of the monopole and dipole time-reversal mirrors are plotted against the off-axis angle in Figs. 17 and 18, respectively. At $kd = 20$, the error is generally less than $\pm 3$ dB between an angle of 6° and 56°. Beyond this angle, the error increases because we are in the region where the imaginary part of the pressure changes sign. Also, there is a significant error on axis (at 0°) due to the finite nature of the radiator, which produces on-axis peaks and nulls in the near field pressure. A similar phenomenon is seen with circular pistons,[15] but this could no doubt be mitigated through the application of suitable apodization.

It is worth noting that the figures shown in this paper can be demonstrated more clearly using animation by plotting

$$\Re(\tilde{p})\cos t - \Im(\tilde{p})\sin t. \tag{44}$$

## VII. CONCLUSIONS

The Kirchhoff-Helmholtz boundary integral has been applied to the case of a point source, where the surface of integration is planar and transparent. As expected, when the plane of integration is infinite, and therefore fully bounds the source, either the monopole or the dipole part (or both) can be used to recreate a sound field outside the boundary that results from sources inside it, provided that the normal velocity or pressure values, respectively, are known at the boundary. Using time reversal, the real part of the field inside the boundary may also be recreated, although the imaginary part is an approximation due to the differing directions of propagation on either side of the source. The resulting phase change in the plane of the source removes the singularity present in the original.

However, it has been shown that the accuracy of the approximation may be improved by using the right combination of the monopole and dipole parts of the boundary integral: A mirror comprising dipole pressure sources gives the best results in the region between the mirror and the location of the original point source, whereas a combination of double-strength monopole velocity sources and anti-phase dipole ones works best on the side of the source furthest from the mirror. Because these superpositions are different, it is not possible to obtain the best possible results everywhere simultaneously, so the choice of transducers will depend on the application.

For a dipole array, the electrostatic loudspeaker has the advantage of being an almost pure pressure source with very little mechanical impedance. Also, a single transducer can act as an array simply by partitioning the electrodes. Indeed, such a loudspeaker has already been used successfully as a form of an acoustic curtain for several decades by employing an analog delay line to feed electrodes in the form of concentric rings in order to replicate the phase and amplitude relationships of a notional incident wave and thus locate a virtual point source behind the loudspeaker.[16] Because of the lack of suitable high-voltage low-power amplifiers, such loudspeakers are still generally driven from stepping-up transformers with the delay line relying on high-voltage passive components. Hence further development of suitable semiconductors is needed in order for the processing to be carried out digitally.

A potential application for the time-reversal principle is in audio-visual entertainment whereby it could be possible to make sounds appear to come from locations in front of the loudspeakers. In order to do this, the phase relationship of the notional incident wave would need to be reversed such that the increasing phase lag with distance from the center of the mirror would become an increasing phase advance. In other words, it would be the reverse of the acoustic-curtain loudspeaker just described, but with a suitable matrix array and digital processing the position of the source could be adjusted electronically.

An important application is in ultrasound where it would be useful to be able to predict the position of the focal point and adjust it electronically. Piezoelectric transducers with oscillating thickness are commonly used because of their near ideal piston movement and high efficiency at very high frequencies.

As increasing processing power is making these kinds of systems more feasible, the search for alternative and affordable kinds of transducers that can fulfil the requirements of multi-loudspeaker systems is an active area of

research with renewed interest in thermo-acoustics[17] and electro-active polymers (artificial muscles).[18]

In this paper, expansions have been derived in order to speed up the computations and these have been applied to finite time-reversal mirrors and acoustic curtains as used for wave field synthesis. The increase in speed is especially apparent in the case of an infinite mirror or curtain. For example, the plots of Fig. 7 and Fig. 8 took less than one-quarter of the time taken using numerical integration. The expansions given in Secs. II–V agree with numerical calculation of the original integrals (see Appendix B). Hence they are rigorous solutions, not approximations.

## APPENDIX A: DERIVATIONS OF EXPANSIONS USED TO CALCULATE FIELDS

### 1. Finite plane circular acoustic curtain or time-reversal mirror using monopole (pressure-gradient) source array

#### a. Pressure field where the distance from the origin to the observation point is greater than the radius of the mirror or curtain

The Green's function of Eq. (23) can be expanded in the same fashion as Eq. (13)

$$g(r,\theta|w_0,\phi_0,z_0)|_{z_0=0} = g(r,\theta|w_0,\phi_0) = \begin{cases} \dfrac{ik}{4\pi}\displaystyle\sum_{p=0}^{\infty}(2p+1)h_p^{(2)}(kr)j_p(kw_0)P_p(\cos\phi_0\sin\theta), & r > w_0 \\ \dfrac{ik}{4\pi}\displaystyle\sum_{p=0}^{\infty}(2p+1)j_p(kr)h_p^{(2)}(kw_0)P_p(\cos\phi_0\sin\theta), & w_0 > r. \end{cases} \tag{A1}$$

Then inserting Eqs. (20) and (A1) in Eq. (22) enables the two integrals in Eq. (22) to be separated as follows:

$$\tilde{p}_M(r,\theta)|_{r>a,d>a} = \frac{ik^3\rho c\tilde{U}_S}{4\pi^2}\sum_{p=0}^{\infty}\sum_{q=0}^{\infty}(2p+1)(q+1)(4q+3)\times\int_0^a j_p(kw_0)j_{2q+1}(kw_0)dw_0\int_0^{2\pi}P_p(\cos\phi_0\sin\theta)d\phi_0$$
$$\times h_p^{(2)}(kr)h_{2q+1}^{(2\backslash 1)}(kd)P_{2q+2}(0). \tag{A2}$$

The Legendre function $P_p$ can be expanded using the following addition theorem[13] (after setting one of the three angles in the original formula to $\pi/2$)

$$P_p(\cos\phi_0\sin\theta) = P_p(0)P_p(\cos\theta) + 2\sum_{q=1}^{\infty}(-1)^q P_p^{-q}(0)P_p^q(\cos\theta)\cos q\phi_0, \tag{A3}$$

which leads to the identity

$$\int_0^{2\pi}P_p(\cos\phi_0\sin\theta)d\phi_0 = 2\pi P_p(0)P_p(\cos\theta) + 2\sum_{q=1}^{\infty}(-1)^q P_p^{-q}(0)P_p^q(\cos\theta)\frac{\sin 2\pi q}{q}$$
$$= 2\pi P_p(0)P_p(\cos\theta), \quad \text{for integral } q. \tag{A4}$$

It is also noted that[13]

$$P_{2p}(0) = \frac{\sqrt{\pi}}{p!\Gamma(1/2-p)} = \frac{(-1)^p\Gamma(p+1/2)}{\sqrt{\pi}p!} \tag{A5}$$

and

$$P_{2p+1}(0) = 0, \tag{A6}$$

so that, after substituting Eqs. (A4)–(A6) in Eq. (A2) and excluding the odd terms, only the radial integral remains as follows:

$$\tilde{p}_M(r,\theta)|_{r>a,d>a} = i\frac{k^3\rho c\tilde{U}_S}{2\pi^2}\sum_{p=0}^{\infty}\sum_{q=0}^{\infty}\frac{(-1)^{p+q}(4p+1)(4q+3)}{p!q!}\Gamma\left(p+\frac{1}{2}\right)\Gamma\left(q+\frac{3}{2}\right)$$
$$\times h_{2p}^{(2)}(kr)h_{2q+1}^{(2\backslash 1)}(kd)P_{2p}(\cos\theta)\int_0^a j_{2p}(kw_0)j_{2q+1}(kw_0)dw_0. \tag{A7}$$

A general solution to the integral over $w_0$ can be written as[19]

$$\int h_m^{(2)}(kw_0)h_n^{(2)}(kw_0)dw_0 = \frac{k^2w_0^2}{k(m+n+1)(n-m)} \times \Big\{h_m^{(2)}(kw_0)h_{n-1}^{(2)}(kw_0) - h_{m-1}^{(2)}(kw_0)h_n^{(2)}(kw_0) - (n-m) \times (h_m^{(2)}(kw_0)h_n^{(2)}(kw_0))/(kw_0)\Big\}, \tag{A8}$$

where $h_m^{(2)}(kw_0)$ is defined in Eq. (15) so that in the case of Eq. (A7) we ignore the $y_m(kw_0)$ terms, leaving just the $j_m(kw_0)$ terms. Hence, after truncating the summation limits to $P$ and $Q$, the final expression for the pressure field becomes

$$\tilde{p}_M(r,\theta)|_{r>a,d>a} = \mp i\frac{k^2\rho c\tilde{U}_S}{4\pi^2}\sum_{p=0}^{P}\sum_{q=0}^{Q}(-1)^{p+q}g_{p,q}^{(M)}h_{2p}^{(2)}(kr) \times h_{2q+1}^{(2\backslash 1)}(kd)f_{p,q}^{(M1)}(ka)P_{2p}(\cos\theta), \tag{A9}$$

where

$$g_{p,q}^{(M)} = \frac{(4p+1)(4q+3)\Gamma(p+1/2)\Gamma(q+3/2)}{p!q!(p+q+1)(2q-2p+1)} \tag{A10}$$

and

$$f_{p,q}^{(M1)}(ka) = k^2a^2\big\{j_{2p}(ka)j_{2q}(ka) - j_{2p-1}(ka)j_{2q+1}(ka) - (2q-2p+1)\big(j_{2p}(ka)j_{2q+1}(ka)\big)/(ka)\big\}. \tag{A11}$$

The solution for $d \le a$ is a little more complicated because the spherical Bessel and Hankel functions have to be exchanged in part of the integral in order to achieve convergence

$$\tilde{p}_M(r,\theta)|_{r>a,0\le d\le a} = i\frac{k^3\rho c\tilde{U}_S}{2\pi^2}\sum_{p=0}^{\infty}\sum_{q=0}^{\infty}\frac{(-1)^{p+q}(4p+1)(4q+3)}{p!q!}\Gamma\left(p+\frac{1}{2}\right)\Gamma\left(q+\frac{3}{2}\right) \times \left(h_{2q+1}^{(2\backslash 1)}(kd)\int_0^d j_{2p}(kw_0)j_{2q+1}(kw_0)dw_0 + j_{2q+1}(kd)\int_d^a j_{2p}(kw_0)h_{2q+1}^{(2\backslash 1)}(kw_0)dw_0\right)h_{2p}^{(2)}(kr)P_{2p}(\cos\theta), \tag{A12}$$

so that, after applying the integral solution of Eq. (A8), together with the following Wronskian:[20]

$$k^2d^2\left(j_{2q}(kd)h_{2q+1}^{(2\backslash 1)}(kd) - j_{2q+1}(kd)h_{2q}^{(2\backslash 1)}(kd)\right) = \mp i, \tag{A13}$$

we obtain

$$\tilde{p}_M(r,\theta)|_{r>a,0\le d\le a} = \mp i\frac{k^2\rho c\tilde{U}_S}{4\pi^2}\sum_{p=0}^{P}\sum_{q=0}^{Q}(-1)^{p+q}g_{p,q}^{(M)}(\pm ij_{2p}(kd) + j_{2q+1}(kd)f_{p,q}^{(M2)}(ka))h_{2p}^{(2)}(kr)P_{2p}(\cos\theta), \tag{A14}$$

where

$$f_{p,q}^{(M2)}(ka) = k^2a^2\Big\{j_{2p}(ka)h_{2q}^{(2\backslash 1)}(ka) - j_{2p-1}(ka)h_{2q+1}^{(2\backslash 1)}(ka) - (2q-2p+1)(j_{2p}(ka)h_{2q+1}^{(2\backslash 1)}(ka))/(ka)\Big\}. \tag{A15}$$

However, this is not the simplest form. Let us now use Eq. (A10) to recast Eq. (A14) into the following form:

$$\tilde{p}_M(r,\theta)|_{r>a,0\le d\le a} = i\frac{k\rho c\tilde{U}_S}{8\pi}\left(-2ik\sum_{p=0}^{P}(4p+1)j_{2p}(kd)h_{2p}^{(2)}(kr)P_{2p}(\cos\theta)\times\left\{\sum_{q=0}^{Q}\frac{(-1)^{p+q}(4q+3)\Gamma(p+1/2)\Gamma(q+3/2)}{\pi p!q!(p+q+1)(2q-2p+1)}\right\}\right.$$
$$\left.\mp\frac{2k}{\pi}\sum_{p=0}^{P}\sum_{q=0}^{Q}(-1)^{p+q}g_{p,q}^{(M)}h_{2p}^{(2)}(kr)j_{2q+1}(kd)f_{p,q}^{(M2)}(ka)P_{2p}(\cos\theta)\right), \tag{A16}$$

which is simplified by applying the following identity:

$$1=\sum_{q=0}^{\infty}\frac{(-1)^{p+q}(4q+3)\Gamma(p+1/2)\Gamma(q+3/2)}{\pi p!q!(p+q+1)(2q-2p+1)} \tag{A17}$$

to the term in braces, which can be proved by exchanging $p$ and $q$ in Eq. (A26) and letting $\theta=0$ so that $P_{2q}(\cos\theta)=P_{2p+1}(\cos\theta)=1$.[13] Hence

$$\tilde{p}_M(r,\theta)|_{r>a,0\le d\le a} = i\frac{k\rho c\tilde{U}_S}{8\pi}\left(-2ik\sum_{p=0}^{P}(4p+1)j_{2p}(kd)h_{2p}^{(2)}(kr)P_{2p}(\cos\theta)\right.$$
$$\left.\mp\frac{2k}{\pi}\sum_{p=0}^{P}\sum_{q=0}^{Q}(-1)^{p+q}g_{p,q}^{(M)}h_{2p}^{(2)}(kr)j_{2q+1}(kd)f_{p,q}^{(M2)}(ka)P_{2p}(\cos\theta)\right). \tag{A18}$$

The single expansion in $p$ only contains odd terms. Noting that $P_p(x)=(-1)^p\,P_p(-x)$, we can write the following expansion containing both odd and even terms:

$$\tilde{p}_M(r,\theta)|_{r>a,0\le d\le a} = i\frac{k\rho c\tilde{U}_S}{8\pi}\left(-ik\sum_{p=0}^{\infty}(2p+1)j_p(kd)h_p^{(2)}(kr)\left(P_p(-\cos\theta)+P_p(\cos\theta)\right)\right.$$
$$\left.\mp\frac{2k}{\pi}\sum_{p=0}^{\infty}\sum_{q=0}^{\infty}(-1)^{p+q}g_{p,q}^{(M)}h_{2p}^{(2)}(kr)j_{2q+1}(kd)f_{p,q}^{(M2)}(ka)P_{2p}(\cos\theta)\right). \tag{A19}$$

Using the identity of Eq. (13) and truncating the summation limits to $P$ and $Q$, this simplifies further to

$$\tilde{p}_M(r,\theta)|_{r>a,0\le d\le a} = i\frac{k\rho c\tilde{U}_S}{8\pi}\left\{\left(\frac{e^{-ikr_0}}{r_0}+\frac{e^{-ikr_1}}{r_1}\right)\mp\frac{2k}{\pi}\sum_{p=0}^{P}\sum_{q=0}^{Q}(-1)^{p+q}\times g_{p,q}^{(M)}h_{2p}^{(2)}(kr)j_{2q+1}(kd)f_{p,q}^{(M2)}(ka)P_{2p}(\cos\theta)\right\}, \tag{A20}$$

where $r_0^2=r^2+d^2+2rd|\cos\theta|$ and $r_1^2=r^2+d^2-2rd|\cos\theta|$.

### 2. Pressure field where the distance from the origin to the observation point is less than the radius of the mirror or curtain

In order to achieve convergence in the region $r\le a$, we simply exchange the spherical Bessel and Hankel functions in Eq. (A7) as follows:

$$\tilde{p}_M(r,\theta)|_{0\le r\le a,d>a} = i\frac{k^3\rho c\tilde{U}_S}{2\pi^2}\sum_{p=0}^{\infty}\sum_{q=0}^{\infty}\frac{(-1)^{p+q}(4p+1)(4q+3)}{p!q!}\Gamma\left(p+\frac{1}{2}\right)\Gamma\left(q+\frac{3}{2}\right)$$
$$\times\left(h_{2p}^{(2)}(kr)\int_0^r j_{2p}(kw_0)j_{2q+1}(kw_0)dw_0+j_{2p}(kr)\int_r^a h_{2p}^{(2)}(kw_0)j_{2q+1}(kw_0)dw_0\right)\times h_{2q+1}^{(2\backslash 1)}(kd)P_{2p}(\cos\theta), \tag{A21}$$

so that, after applying the integral solution of Eq. (A8), together with the following Wronskian:

$$k^2r^2\left(j_{2p}(kr)h^{(2)}_{2p-1}(kr)-j_{2p-1}(kr)h^{(2)}_{2p}(kr)\right)=i \tag{A22}$$

we obtain

$$\tilde{p}_M(r,\theta)|_{0\le r\le a,d>a}=\mp i\frac{k^2\rho c\tilde{U}_S}{4\pi^2}\sum_{p=0}^{\infty}\sum_{q=0}^{\infty}(-1)^{p+q}g^{(M)}_{p,q}(-ij_{2q+1}(kr)+j_{2p}(kr)f^{(M3)}_{p,q}(ka))h^{(2\backslash 1)}_{2q+1}(kd)P_{2p}(\cos\theta), \tag{A23}$$

where

$$f^{(M3)}_{p,q}(ka)=k^2a^2\left\{h^{(2)}_{2p}(ka)j_{2q}(ka)-h^{(2)}_{2p-1}(ka)j_{2q+1}(ka)-(2q-2p+1)(h^{(2)}_{2p}(ka)j_{2q+1}(ka))/(ka)\right\}. \tag{A24}$$

However, this is not the simplest form. Let us now use Eq. (A10) to recast Eq. (A23) into the following form:

$$\begin{aligned}\tilde{p}_M(r,\theta)|_{0\le r\le a,d>a}=i\frac{k\rho c\tilde{U}_S}{8\pi}\Bigg(&\pm 2ik\sum_{q=0}^{\infty}(4q+3)j_{2q+1}(kr)h^{(2\backslash 1)}_{2q+1}(kd)\\&\times\left\{\sum_{p=0}^{\infty}\frac{(-1)^{p+q}(4p+1)\Gamma(p+1/2)\Gamma(q+3/2)}{\pi p!q!(p+q+1)(2q-2p+1)}P_{2p}(\cos\theta)\right\}\\&\mp\frac{2k}{\pi}\sum_{p=0}^{\infty}\sum_{q=0}^{\infty}(-1)^{p+q}g^{(M)}_{p,q}j_{2p}(kr)h^{(2\backslash 1)}_{2q+1}(kd)f^{(M3)}_{p,q}(ka)P_{2p}(\cos\theta)),\end{aligned} \tag{A25}$$

which is simplified by applying the following identity:[13]

$$P_{2q+1}(\cos\theta)=\sum_{p=0}^{\infty}\frac{(-1)^{p+q}(4p+1)\Gamma(p+1/2)\Gamma(q+3/2)}{\pi p!q!(p+q+1)(2q-2p+1)}P_{2p}(\cos\theta),\quad 0\le\theta\le\frac{\pi}{2} \tag{A26}$$

to the term in braces. It is derived from

$$P_{2q+1}(\cos\theta)=\sum_{p=0}^{\infty}A_{p,q}P_{2p}(\cos\theta), \tag{A27}$$

where

$$A_{p,q}=\frac{\int_0^{\pi/2}P_{2q+1}(\cos\theta)P_{2p}(\cos\theta)\sin\theta d\theta}{\int_0^{\pi/2}P_{2p}(\cos\theta)P_{2p}(\cos\theta)\sin\theta d\theta}. \tag{A28}$$

Hence

$$\begin{aligned}\tilde{p}_M(r,\theta)|_{0\le r\le a,d>a}=i\frac{k\rho c\tilde{U}_S}{8\pi}\Bigg(&\pm 2ik\sum_{q=0}^{\infty}(4q+3)j_{2q+1}(kr)h^{(2\backslash 1)}_{2q+1}(kd)P_{2q+1}(\cos\theta)\\&\mp\frac{2k}{\pi}\sum_{p=0}^{\infty}\sum_{q=0}^{\infty}(-1)^{p+q}g^{(M)}_{p,q}j_{2p}(kr)h^{(2\backslash 1)}_{2q+1}(kd)f^{(M3)}_{p,q}(ka)P_{2p}(\cos\theta)\Bigg).\end{aligned} \tag{A29}$$

The single expansion in $q$ only contains odd terms. Noting that $P_q(x)=(-1)^q P_q(-x)$, we can write the following expansion containing both odd and even terms:

$$\tilde{p}_M(r,\theta)|_{0\le r\le a,d>a} = i\frac{k\rho c\tilde{U}_S}{8\pi}\left(\mp ik\sum_{q=0}^{\infty}(2q+1)j_q(kr)h_q^{(2\backslash 1)}(kd)\left(P_q(-\cos\theta)-P_q(\cos\theta)\right)\right.$$
$$\left.\mp\frac{2k}{\pi}\sum_{p=0}^{\infty}\sum_{q=0}^{\infty}(-1)^{p+q}g_{p,q}^{(M)}j_{2p}(kr)h_{2q+1}^{(2\backslash 1)}(kd)f_{p,q}^{(M3)}(ka)P_{2p}(\cos\theta)\right). \tag{A30}$$

Using the identity of Eq. (13) and truncating the summation limits to $P$ and $Q$, this simplifies further to

$$\tilde{p}_M(r,\theta)|_{0\le r\le a,d>a} = i\frac{k\rho c\tilde{U}_S}{8\pi}\left\{\left(\frac{e^{\mp ikr_0}}{r_0}-\frac{e^{\mp ikr_1}}{r_1}\right)\mp\frac{2k}{\pi}\sum_{p=0}^{P}\sum_{q=0}^{Q}(-1)^{p+q}\times g_{p,q}^{(M)}j_{2p}(kr)h_{2q+1}^{(2\backslash 1)}(kd)f_{p,q}^{(M3)}(ka)P_{2p}(\cos\theta)\right\}, \tag{A31}$$

where $r_0^2 = r^2+d^2+2rd|\cos\theta|$ and $r_1^2 = r^2+d^2-2rd|\cos\theta|$.

The solution for $d\le a$ is a little more complicated because the spherical Bessel and Hankel functions have to be exchanged in part of the integral in order to achieve convergence. First, for $r\le d$, we have

$$\tilde{p}_M(r,\theta)|_{0\le r\le d,0\le d\le a} = i\frac{k^3\rho c\tilde{U}_S}{2\pi^2}\sum_{p=0}^{\infty}\sum_{q=0}^{\infty}\frac{(-1)^{p+q}(4p+1)(4q+3)}{p!q!}\Gamma\left(p+\frac{1}{2}\right)\Gamma\left(q+\frac{3}{2}\right)$$
$$\times\left(h_{2p}^{(2)}(kr)h_{2q+1}^{(2\backslash 1)}(kd)\int_0^r j_{2p}(kw_0)j_{2q+1}(kw_0)dw_0 + j_{2p}(kr)h_{2q+1}^{(2\backslash 1)}(kd)\int_r^d h_{2p}^{(2)}(kw_0)j_{2q+1}(kw_0)dw_0\right.$$
$$\left.+\,j_{2p}(kr)j_{2q+1}(kd)\int_d^a h_{2p}^{(2)}(kw_0)h_{2q+1}^{(2\backslash 1)}(kw_0)dw_0\right)\times P_{2p}(\cos\theta), \tag{A32}$$

so that, after applying the integral solution of Eq. (A8), together with the Wronskians of Eqs. (A13) and (A22), and truncating the summation limits to $P$ and $Q$, the final expression for the pressure field becomes

$$\tilde{p}_M(r,\theta)|_{0\le r\le d,0\le d\le a} = \mp i\frac{k^2\rho c\tilde{U}_S}{4\pi^2}\sum_{p=0}^{P}\sum_{q=0}^{Q}(-1)^{p+q}g_{p,q}^{(M)}(\pm ij_{2p}(kr)h_{2p}^{(2)}(kd)$$
$$-ij_{2q+1}(kr)h_{2q+1}^{(2\backslash 1)}(kd)+j_{2p}(kr)j_{2q+1}(kd)f_{p,q}^{(M4)})P_{2p}(\cos\theta), \tag{A33}$$

where

$$f_{p,q}^{(M4)}(ka) = k^2a^2\left\{h_{2p}^{(2)}(ka)h_{2q}^{(2\backslash 1)}(ka)-h_{2p-1}^{(2)}(ka)h_{2q+1}^{(2\backslash 1)}(ka)-(2q-2p+1)(h_{2p}^{(2)}(ka)h_{2q+1}^{(2\backslash 1)}(ka))/(ka)\right\}. \tag{A34}$$

Second, for $r>d$, we have

$$\tilde{p}_M(r,\theta)|_{d<r\le a,0\le d\le a} = i\frac{k^3\rho c\tilde{U}_S}{2\pi^2}\sum_{p=0}^{\infty}\sum_{q=0}^{\infty}\frac{(-1)^{p+q}(4p+1)(4q+3)}{p!q!}\Gamma\left(p+\frac{1}{2}\right)\Gamma\left(q+\frac{3}{2}\right)$$
$$\times\left(h_{2p}^{(2)}(kr)h_{2q+1}^{(2\backslash 1)}(kd)\int_0^d j_{2p}(kw_0)j_{2q+1}(kw_0)dw_0 + h_{2p}^{(2)}(kr)j_{2q+1}(kd)\int_d^r j_{2p}(kw_0)h_{2q+1}^{(2\backslash 1)}(kw_0)dw_0\right.$$
$$\left.+\,j_{2p}(kr)j_{2q+1}(kd)\int_r^a h_{2p}^{(2)}(kw_0)h_{2q+1}^{(2\backslash 1)}(kw_0)dw_0\right)\times P_{2p}(\cos\theta), \tag{A35}$$

so that, after applying the integral solution of Eq. (A8), together with the Wronskians of Eqs. (A13) and (A22), and truncating the summation limits to $P$ and $Q$, the final expression for the pressure field becomes

$$\tilde{p}_M(r,\theta)|_{d\le r\le a,0\le d\le a} = \mp i\frac{k^2\rho c\tilde{U}_S}{4\pi^2}\sum_{p=0}^{P}\sum_{q=0}^{Q}(-1)^{p+q}g_{p,q}^{(M)}(\pm ij_{2p}(kd)h_{2p}^{(2)}(kr)$$
$$-ij_{2q+1}(kd)h_{2q+1}^{(2\backslash 1)}(kr)+j_{2p}(kr)j_{2q+1}(kd)f_{p,q}^{(M4)}(ka))P_{2p}(\cos\theta), \tag{A36}$$

where $f_{p,q}^{(M4)}(ka)$ is given by Eq. (A34). Again, using similar arguments to those above, this can be simplified to

$$\tilde{p}_M(r,\theta)|_{0\le r\le a,0\le d\le a} = i\frac{k\rho c\tilde{U}_S}{8\pi}\left\{\frac{e^{\mp ikr_0}}{r_0}-\frac{e^{\mp ikr_1}}{r_1}+\frac{e^{-ikr_0}}{r_0}+\frac{e^{-ikr_1}}{r_1}\mp\frac{2k}{\pi}\sum_{p=0}^{P}\sum_{q=0}^{Q}(-1)^{p+q}g_{p,q}^{(M)}j_{2p}(kr)\right.$$
$$\left.\times\, j_{2q+1}(kd)f_{p,q}^{(M4)}(ka)P_{2p}(\cos\theta)\right\}. \tag{A37}$$

### 2. Finite plane circular acoustic curtain or time-reversal mirror using dipole (pressure) source array

#### *1. Pressure field where the distance from the origin to the observation point is greater than the radius of the mirror or curtain*

It was shown in a previous paper[10] that, in the case of a uniform driving pressure $\tilde{p}_0$ in the region $0\le w_0\le a$, the following solution may be given to Eq. (32):

$$\tilde{p}_D(r,\theta) = \frac{ik\tilde{p}_0}{\sqrt{\pi}}\sum_{p=0}^{\infty}(-1)^p(4p+3)\frac{\Gamma(p+3/2)}{p!}\times\int_0^a j_{2p+1}(kw_0)dw_0h_{2p+1}^{(2)}(kr)P_{2p+1}(\cos\theta), \tag{A38}$$

where $\tilde{p}_+(w_0) = -\tilde{p}_-(w_0) = \tilde{p}_0/2$. We now replace $\tilde{p}_0$ with the non-uniform pressure distribution $\tilde{p}_S(w_0,0)$ so that

$$\tilde{p}_D(r,\theta)|_{r>a,d>a} = \frac{ik}{\sqrt{\pi}}\sum_{p=0}^{\infty}(-1)^p(4p+3)\frac{\Gamma(p+3/2)}{p!}\times\int_0^a\tilde{p}_S(w_0)|_{d>w_0}j_{2p+1}(kw_0)dw_0\times h_{2p+1}^{(2)}(kr)P_{2p+1}(\cos\theta), \tag{A39}$$

which after inserting Eq. (30) can be written

$$\tilde{p}_D(r,\theta)|_{r>a,d>a} = -i\frac{k^3\rho c\tilde{U}_S}{4\pi^2}\sum_{p=0}^{\infty}\sum_{q=0}^{\infty}\frac{(-1)^{p+q}(4p+3)(4q+1)\Gamma(p+3/2)\Gamma(q+1/2)}{p!q!}$$
$$\times\int_0^a j_{2q}(kw_0)j_{2p+1}(kw_0)dw_0h_{2q}^{(2\backslash 1)}(kd)h_{2p+1}^{(2)}(kr)P_{2p+1}(\cos\theta), \tag{A40}$$

so that, after applying the integral solution of Eq. (A8) and truncating the summation limits to $P$ and $Q$, the final expression for the pressure field becomes

$$\tilde{p}_D(r,\theta)|_{r>a,d>a} = -i\frac{k^2\rho c\tilde{U}_S}{4\pi^2}\sum_{p=0}^{P}\sum_{q=0}^{Q}(-1)^{p+q}g_{p,q}^{(D)}h_{2p+1}^{(2)}(kr)\times h_{2q}^{(2\backslash 1)}(kd)f_{p,q}^{(D1)}(ka)P_{2p+1}(\cos\theta), \tag{A41}$$

where

$$g_{p,q}^{(D)} = \frac{(4p+3)(4q+1)\Gamma(p+3/2)\Gamma(q+1/2)}{p!q!(p+q+1)(2p-2q+1)} \tag{A42}$$

and

$$f_{p,q}^{(D1)}(ka) = k^2a^2\left\{j_{2p}(ka)j_{2q}(ka)-j_{2p+1}(ka)j_{2q-1}(ka)-(2p-2q+1)\left(j_{2p+1}(ka)j_{2q}(ka)\right)/(ka)\right\}. \tag{A43}$$

The solution for $d\le a$ is a little more complicated because the spherical Bessel and Hankel functions have to be exchanged in part of the integral in order to achieve convergence

$$\tilde{p}_D(r,\theta)|_{r>a,0\le d\le a} = -i\frac{k^3\rho c\tilde{U}_S}{2\pi^2}\sum_{p=0}^{\infty}\sum_{q=0}^{\infty}\frac{(-1)^{p+q}(4p+3)(4q+1)\Gamma(p+3/2)\Gamma(q+1/2)}{p!q!}$$
$$\times\left(h_{2q}^{(2\backslash 1)}(kd)\int_0^d j_{2q}(kw_0)j_{2p+1}(kw_0)dw_0+j_{2q}(kd)\int_d^a h_{2q}^{(2\backslash 1)}(kw_0)j_{2p+1}(kw_0)dw_0\right)h_{2p+1}^{(2)}(kr)P_{2p+1}(\cos\theta), \tag{A44}$$

so that, after applying the integral solution of Eq. (A8), together with the Wronskian of Eq. (A13), we obtain

$$\tilde{p}_D(r,\theta)|_{r>a,0\le d\le a} = -i\frac{k^2\rho c\tilde{U}_S}{4\pi^2}\sum_{p=0}^{\infty}\sum_{q=0}^{\infty}(-1)^{p+q}g_{p,q}^{(D)}\left(\mp ij_{2p+1}(kd)+j_{2q}(kd)f_{p,q}^{(D2)}(ka)\right)h_{2p+1}^{(2)}(kr)P_{2p+1}(\cos\theta), \tag{A45}$$

where

$$f_{p,q}^{(D2)}(ka) = k^2a^2\left\{j_{2p}(ka)h_{2q}^{(2\backslash 1)}(ka) - j_{2p+1}(ka)h_{2q-1}^{(2\backslash 1)}(ka) - (2p-2q+1)\left(j_{2p+1}(ka)h_{2q}^{(2\backslash 1)}(ka)\right)\Big/(ka)\right\}. \tag{A46}$$

However, this is not the simplest form. Let us now use Eq. (A42) to recast Eq. (A45) into the following form:

$$\begin{aligned}\tilde{p}_D(r,\theta)|_{r>a,0\le d\le a} = -i\frac{k\rho c\tilde{U}_S}{8\pi}\Bigg(&\mp 2ik\sum_{p=0}^{\infty}(4p+3)j_{2p+1}(kd)h_{2p+1}^{(2)}(kr)P_{2p+1}(\cos\theta)\\ &\times\left\{\sum_{q=0}^{\infty}\frac{(-1)^{p+q}(4q+1)\Gamma(p+3/2)\Gamma(q+1/2)}{\pi p!q!(p+q+1)(2p-2q+1)}\right\}\\ &+\frac{2k}{\pi}\sum_{p=0}^{\infty}\sum_{q=0}^{\infty}(-1)^{p+q}g_{p,q}^{(D)}h_{2p+1}^{(2)}(kr)j_{2q}(kd)f_{p,q}^{(D2)}(ka)P_{2p+1}(\cos\theta)\Bigg),\end{aligned} \tag{A47}$$

which is simplified by applying the following identity:

$$1 = \sum_{q=0}^{\infty}\frac{(-1)^{p+q}(4q+1)\Gamma(p+3/2)\Gamma(q+1/2)}{\pi p!q!(p+q+1)(2p-2q+1)} \tag{A48}$$

to the term in braces, which can be proved by exchanging $p$ and $q$ in Eq. (A26) and letting $\theta=0$ so that $P_{2q+1}(\cos\theta)=P_{2p}(\cos\theta)=1$.[13] Hence

$$\begin{aligned}\tilde{p}_D(r,\theta)|_{r>a,0\le d\le a} = -i\frac{k\rho c\tilde{U}_S}{8\pi}\Bigg(&\mp 2ik\sum_{p=0}^{\infty}(4p+3)j_{2p+1}(kd)h_{2p+1}^{(2)}(kr)P_{2p+1}(\cos\theta)\\ &+\frac{2k}{\pi}\sum_{p=0}^{\infty}\sum_{q=0}^{\infty}(-1)^{p+q}g_{p,q}^{(D)}h_{2p+1}^{(2)}(kr)j_{2q}(kd)f_{p,q}^{(D2)}(ka)P_{2p+1}(\cos\theta)\Bigg).\end{aligned} \tag{A49}$$

The single expansion in $p$ only contains odd terms. Noting that $P_p(x)=(-1)^p\,P_p(-x)$, we can write the following expansion containing both odd and even terms:

$$\begin{aligned}\tilde{p}_D(r,\theta)|_{r>a,0\le d\le a} = i\frac{k\rho c\tilde{U}_S}{8\pi}\Bigg(&\pm ik\sum_{p=0}^{\infty}(2p+1)j_p(kd)h_p^{(2)}(kr)(P_p(-\cos\theta)+P_p(\cos\theta))\\ &-\frac{2k}{\pi}\sum_{p=0}^{\infty}\sum_{q=0}^{\infty}(-1)^{p+q}g_{p,q}^{(D)}h_{2p+1}^{(2)}(kr)j_{2q}(kd)f_{p,q}^{(D2)}(ka)P_{2p+1}(\cos\theta)\Bigg).\end{aligned} \tag{A50}$$

Using the identity of Eq. (13) and truncating the summation limits to $P$ and $Q$, this simplifies further to

$$\begin{aligned}\tilde{p}_D(r,\theta)|_{r>a,0\le d\le a} = i\frac{k\rho c\tilde{U}_S}{8\pi}\Bigg\{&\pm\mathrm{sgn}(\cos\theta)\left(\frac{e^{-ikr_0}}{r_0}-\frac{e^{-ikr_1}}{r_1}\right)-\frac{2k}{\pi}\sum_{p=0}^{P}\sum_{q=0}^{Q}(-1)^{p+q}\\ &\times g_{p,q}^{(D)}h_{2p+1}^{(2)}(kr)j_{2q}(kd)f_{p,q}^{(D2)}(ka)P_{2p+1}(\cos\theta)\Bigg\},\end{aligned} \tag{A51}$$

where $r_0^2 = r^2+d^2+2rd|\cos\theta|$ and $r_1^2 = r^2+d^2-2rd|\cos\theta|$.

### 2. Pressure field where the distance from the origin to the observation point is less than the radius of the mirror or curtain

In order to achieve convergence in the region $r \le a$, we simply exchange the spherical Bessel and Hankel functions in Eq. (A40) as follows:

$$\tilde{p}_D(r,\theta)|_{0\le r\le a, d>a} = -i\frac{k^3\rho c\tilde{U}_S}{2\pi^2}\sum_{p=0}^{\infty}\sum_{q=0}^{\infty}\frac{(-1)^{p+q}(4p+3)(4q+1)\Gamma(p+3/2)\Gamma(q+1/2)}{p!q!} \times\left(h_{2p+1}^{(2)}(kr)\int_0^r j_{2p+1}(kw_0)j_{2q}(kw_0)dw_0 + j_{2p+1}(kr)\int_r^a h_{2p+1}^{(2)}(kw_0)j_{2q}(kw_0)dw_0\right)h_{2q}^{(2\backslash 1)}(kd)P_{2p+1}(\cos\theta), \tag{A52}$$

so that, after applying the integral solution of Eq. (A8), together with the Wronskian of Eq. (A22), we obtain

$$\tilde{p}_D(r,\theta)|_{0\le r\le a, d>a} = -i\frac{k^2\rho c\tilde{U}_S}{4\pi^2}\sum_{p=0}^{\infty}\sum_{q=0}^{\infty}(-1)^{p+q}g_{p,q}^{(D)}\left(ij_{2q}(kr)+j_{2p+1}(kr)f_{p,q}^{(D3)}(ka)\right)h_{2q}^{(2\backslash 1)}(kd)P_{2p+1}(\cos\theta), \tag{A53}$$

where

$$f_{p,q}^{(D3)}(ka) = k^2a^2\left\{h_{2p}^{(2)}(ka)j_{2q}(ka) - h_{2p+1}^{(2)}(ka)j_{2q-1}(ka) - (2p-2q+1)\left(h_{2p+1}^{(2)}(ka)j_{2q}(ka)\right)\Big/(ka)\right\}. \tag{A54}$$

However, this is not the simplest form. Let us now use Eq. (A42) to recast Eq. (A53) into the following form:

$$\tilde{p}_D(r,\theta)|_{0\le r\le a, d>a} = i\frac{k\rho c\tilde{U}_S}{8\pi}\left(-2ik\sum_{q=0}^{\infty}(4q+1)j_{2q}(kr)h_{2q}^{(2\backslash 1)}(kd) \times\left\{\sum_{p=0}^{\infty}\frac{(-1)^{p+q}(4p+3)\Gamma(p+3/2)\Gamma(q+1/2)}{\pi p!q!(p+q+1)(2p-2q+1)}P_{2p+1}(\cos\theta)\right\} - \frac{2k}{\pi}\sum_{p=0}^{\infty}\sum_{q=0}^{\infty}(-1)^{p+q}g_{p,q}^{(D)}j_{2p+1}(kr)h_{2q}^{(2\backslash 1)}(kd)f_{p,q}^{(D3)}(ka)P_{2p+1}(\cos\theta)\right), \tag{A55}$$

which is simplified by applying the following identity:[13]

$$\mathrm{sgn}(\cos\theta)P_{2q}(\cos\theta) = \sum_{p=0}^{\infty}\frac{(-1)^{p+q}(4p+3)\Gamma(p+3/2)\Gamma(q+1/2)}{\pi p!q!(p+q+1)(2p-2q+1)}P_{2p+1}(\cos\theta) \tag{A56}$$

to the term in braces. It is derived from

$$\mathrm{sgn}(\cos\theta)P_{2q}(\cos\theta) = \sum_{p=0}^{\infty}A_{p,q}P_{2p+1}(\cos\theta), \tag{A57}$$

where

$$A_{p,q} = \frac{\int_0^{\pi/2}P_{2q}(\cos\theta)P_{2p+1}(\cos\theta)\sin\theta d\theta}{\int_0^{\pi/2}P_{2p+1}(\cos\theta)P_{2p+1}(\cos\theta)\sin\theta d\theta}. \tag{A58}$$

Hence

$$\tilde{p}_D(r,\theta)|_{0\le r\le a,d>a} = i\frac{k\rho c\tilde{U}_S}{8\pi}\left(-2ik\sum_{q=0}^{\infty}(4q+1)j_{2q}(kr)h_{2q}^{(2\backslash 1)}(kd)P_{2q}(\cos\theta)\right.$$
$$\left.-\frac{2k}{\pi}\sum_{p=0}^{\infty}\sum_{q=0}^{\infty}(-1)^{p+q}g_{p,q}^{(D)}j_{2p+1}(kr)h_{2q}^{(2\backslash 1)}(kd)f_{p,q}^{(D3)}(ka)P_{2p+1}(\cos\theta)\right). \tag{A59}$$

The single expansion in $q$ only contains odd terms. Noting that $P_q(x)=(-1)^q\,P_q(-x)$, we can write the following expansion containing both odd and even terms:

$$\tilde{p}_D(r,\theta)|_{0\le r\le a,d>a} = i\frac{k\rho c\tilde{U}_S}{8\pi}\left(-ik\sum_{q=0}^{\infty}(2q+1)j_q(kr)h_q^{(2\backslash 1)}(kd)\big(P_q(-\cos\theta)-P_q(\cos\theta)\big)\right.$$
$$\left.-\frac{2k}{\pi}\sum_{p=0}^{\infty}\sum_{q=0}^{\infty}(-1)^{p+q}g_{p,q}^{(D)}j_{2p+1}(kr)h_{2q}^{(2\backslash 1)}(kd)f_{p,q}^{(D3)}(ka)P_{2p+1}(\cos\theta)\right). \tag{A60}$$

Using the identity of Eq. (13) and truncating the summation limits to $P$ and $Q$, this simplifies further to

$$\tilde{p}_D(r,\theta)|_{0\le r\le a,d>a} = i\frac{k\rho c\tilde{U}_S}{8\pi}\left\{\pm\mathrm{sgn}(\cos\theta)\left(\frac{e^{\mp ikr_0}}{r_0}+\frac{e^{\mp ikr_1}}{r_1}\right)-\frac{2k}{\pi}\sum_{p=0}^{P}\sum_{q=0}^{Q}(-1)^{p+q}\right.$$
$$\left.\times\, g_{p,q}^{(D)}j_{2p+1}(kr)h_{2q}^{(2\backslash 1)}(kd)f_{p,q}^{(D3)}(ka)P_{2p+1}(\cos\theta)\right\}, \tag{A61}$$

where $r_0^2=r^2+d^2+2rd|\cos\theta|$ and $r_1^2=r^2+d^2-2rd|\cos\theta|$.

The solution for $d\le a$ is a little more complicated because the spherical Bessel and Hankel functions have to be exchanged in part of the integral in order to achieve convergence. First, for $r\le d$, we have

$$\tilde{p}_D(r,\theta)|_{0\le r\le d,0\le d\le a} = -1\frac{k^3\rho c\tilde{U}_S}{4\pi^2}\sum_{p=0}^{\infty}\sum_{q=0}^{\infty}\frac{(-1)^{p+q}(4q+1)(4p+3)\Gamma(p+3/2)\Gamma(q+1/2)}{p!q!}$$
$$\times\left(h_{2p+1}^{(2)}(kr)h_{2q}^{(2\backslash 1)}(kd)\int_0^r j_{2q}(kw_0)j_{2p+1}(kw_0)dw_0+j_{2p+1}(kr)h_{2q}^{(2\backslash 1)}(kd)\int_r^d h_{2p+1}^{(2)}(kw_0)j_{2q}(kw_0)dw_0\right.$$
$$\left.+j_{2p+1}(kr)j_{2q}(kd)\int_d^a h_{2p+1}^{(2)}(kw_0)h_{2q}^{(2\backslash 1)}(kw_0)dw_0\right)P_{2p+1}(\cos\theta), \tag{A62}$$

so that, after applying the integral solution of Eq. (A8), together with the Wronskians of Eqs. (A13) and (A22), and truncating the summation limits to $P$ and $Q$, the final expression for the pressure field becomes

$$\tilde{p}_D(r,\theta)|_{0\le r\le d,0\le d\le a} = -i\frac{k^2\rho c\tilde{U}_S}{8\pi^2}\sum_{p=0}^{P}\sum_{q=0}^{Q}(-1)^{p+q}g_{p,q}^{(D)}$$
$$\times\,(ij_{2q}(kr)h_{2q}^{(2\backslash 1)}(kd)\mp ij_{2p+1}(kr)h_{2p+1}^{(2)}(kd)+j_{2p+1}(kr)j_{2q}(kd)f_{p,q}^{(D4)}(ka))P_{2p+1}(\cos\theta), \tag{A63}$$

where

$$f_{p,q}^{(D4)}(ka)=k^2a^2\left\{h_{2p}^{(2)}(ka)h_{2q}^{(2\backslash 1)}(ka)-h_{2p+1}^{(2)}(ka)h_{2q-1}^{(2\backslash 1)}(ka)-(2p-2q+1)\left(h_{2p+1}^{(2)}(ka)h_{2q}^{(2\backslash 1)}(ka)\right)\Big/(ka)\right\}. \tag{A64}$$

Second, for $r>d$, we have

$$\tilde{p}_D(r,\theta)|_{d<r\le a,0\le d\le a} = -i\frac{k^3\rho c\tilde{U}_S}{4\pi^3}\sum_{p=0}^{\infty}\sum_{q=0}^{\infty}\frac{(-1)^{p+q}(4p+3)(4q+1)\Gamma(p+3/2)\Gamma(q+1/2)}{p!q!}$$
$$\times\left(h_{2p+1}^{(2)}(kr)h_{2q}^{(2\backslash 1)}(kd)\int_0^d j_{2p+1}(kw_0)j_{2q}(kw_0)dw_0 + h_{2p+1}^{(2)}(kr)j_{2q}(kd)\int_d^r j_{2p+1}(kw_0)h_{2q}^{(2\backslash 1)}(kw_0)dw_0\right.$$
$$\left.+ j_{2p+1}(kr)j_{2q}(kd)\int_r^a h_{2p+1}^{(2)}(kw_0)h_{2q}^{(2\backslash 1)}(kw_0)dw_0\right)P_{2p+1}(\cos\theta), \tag{A65}$$

so that, after applying the integral solution of Eq. (A8), together with the Wronskians of Eqs. (A13) and (A22), and truncating the summation limits to $P$ and $Q$, the final expression for the pressure field becomes

$$\tilde{p}_D(r,\theta)|_{d\le r\le a,0\le d\le a} = -i\frac{k^2\rho c\tilde{U}_S}{8\pi^2}\sum_{p=0}^{P}\sum_{q=0}^{Q}(-1)^{p+q}g_{p,q}^{(D)}$$
$$\times\left(ij_{2q}(kd)h_{2q}^{(2\backslash 1)}(kr)\mp ij_{2p+1}(kd)h_{2p+1}^{(2)}(kr)+j_{2p+1}(kr)j_{2q}(kd)f_{p,q}^{(D4)}(ka)\right)P_{2p+1}(\cos\theta), \tag{A66}$$

where $f_{p,q}^{(D4)}(ka)$ is given by Eq. (A64). Again, using similar arguments to those above, this can be simplified to

$$\tilde{p}_D(r,\theta)|_{0\le r\le a,0\le d\le a} = i\frac{k\rho c\tilde{U}_S}{8\pi}\left\{\pm\mathrm{sgn}(\cos\theta)\left(\frac{e^{\mp ikr_0}}{r_0}+\frac{e^{\mp ikr_1}}{r_1}+\frac{e^{-ikr_0}}{r_0}-\frac{e^{-ikr_1}}{r_1}\right)\right.$$
$$\left.-\frac{2k}{\pi}\sum_{p=0}^{P}\sum_{q=0}^{Q}(-1)^{p+q}g_{p,q}j_{2p+1}(kr)j_{2q}(kd)f_{p,q}^{(D4)}(ka)P_{2p+1}(\cos\theta)\right\}. \tag{A67}$$

## APPENDIX B: ALTERNATE FORMULAS FOR CALCULATING FIELDS USING NUMERICAL INTEGRATION

### 1. Finite plane circular acoustic curtain or time-reversal mirror using monopole (pressure-gradient) source array

This appendix presents the numerical integrals, in cylindrical coordinates, which the authors used to validate the analytical solutions in the form of expansions

$$\tilde{p}_M(w,z) = -2\int_0^{2\pi}\int_0^a \frac{\partial}{\partial z_0}\tilde{p}(w_0,z_0)|_{z_0=0}g(w,\phi,z|w_0,\phi_0,z_0)|_{\varphi=z_0=0}wdwd\phi_0, \tag{B1}$$

where

$$\frac{\partial}{\partial z_0}\tilde{p}(w_0,z_0)|_{z_0=0} = \pm k^2 d\rho c\tilde{U}_S\left(1\pm\frac{1}{ik\sqrt{w_0^2+d^2}}\right)\frac{e^{\mp ik\sqrt{w_0^2+d^2}}}{4\pi(w_0^2+d^2)}, \tag{B2}$$

$$g(w,\phi,z|w_0,\phi_0,z_0) = \frac{e^{-ik\sqrt{w^2+w_0^2-2ww_0\cos(\varphi-\varphi_0)+(z-z_0)^2}}}{4\pi\sqrt{w^2+w_0^2-2ww_0\cos(\phi-\phi_0)+(z-z_0)^2}}. \tag{B3}$$

### 2. Finite plane circular acoustic curtain or time-reversal mirror using dipole (pressure) source array

$$\tilde{p}_D(w,z) = 2\int_0^{2\pi}\int_0^a \tilde{p}(w_0,z_0)|_{z_0=0}\frac{\partial}{\partial z_0}g(w,\phi,z|w_0,\phi_0,z_0)|_{\phi=z_0=0}wdwd\phi_0, \tag{B4}$$

$$\tilde{p}(w_0,z_0) = \mp ik\rho c\tilde{U}_S\frac{e^{\mp ik\sqrt{w_0^2+(d-z_0)^2}}}{4\pi\sqrt{w_0^2+(d-z_0)^2}}, \tag{B5}$$

$$\frac{\partial}{\partial z_0} g(w,\phi,z|w_0,\phi_0,z_0)|_{\phi=z_0=0} = ikz\left(1+\frac{1}{ik\sqrt{w^2+w_0^2-2ww_0\cos\phi_0+z^2}}\right)\times\frac{e^{-ik\sqrt{w^2+w_0^2-2ww_0\cos\phi_0+z^2}}}{4\pi(w^2+w_0^2-2ww_0\cos\phi_0+z^2)}. \tag{B6}$$

## APPENDIX C: PASSIVE ACOUSTIC SINK

The solution to the following homogeneous Helmholtz spherical wave equation

$$\left(\frac{\partial^2}{\partial r^2}+\frac{2}{r}\cdot\frac{\partial}{\partial r}+k^2\right)\tilde{p}(r)=0 \tag{C1}$$

is given by

$$\tilde{p}(r)=\tilde{p}_+\frac{e^{-ikr}}{r}+\tilde{p}_-\frac{e^{ikr}}{r}, \tag{C2}$$

where $\tilde{p}_+$ is the strength of the diverging wave and $\tilde{p}_-$ is that of the converging one. The velocity in the direction toward the origin is given by

$$\begin{aligned}\tilde{u}(r) &= \frac{1}{ik\rho c}\tilde{p}(r)\\ &= \frac{\tilde{p}_+}{\rho c}\left(\frac{i}{kr}-1\right)\frac{e^{-ikr}}{r}+\frac{\tilde{p}_-}{\rho c}\left(\frac{i}{kr}+1\right)\frac{e^{ikr}}{r}.\end{aligned} \tag{C3}$$

If we have a sphere of radius $R$ with an anechoic surface impedance of $\rho c$, we can write the boundary condition

$$\frac{\tilde{p}(R)}{\tilde{u}(R)}=\rho c \tag{C4}$$

so that

$$\tilde{p}_+ - \frac{e^{2ikR}}{1+2ikR}\tilde{p}_-. \tag{C5}$$

Hence, when $kR$ is very large or the wavelength is very small in comparison to the radius of the sphere, $\tilde{p}_+$ (which is the strength of the reflected wave) becomes vanishingly small and we are left with the converging wave without any reflections. However, this only holds for small wavelengths. Another problem for large wavelengths is that if such a sphere were fabricated from a piece of porous absorbent material, the air within it would act as compliance and the resistive part of the impedance would be small. In other words, it would only be substantially resistive for smaller wavelengths and the resistance would be less than one-half of the flow resistance of the material.


[1]http://www.holophony.net/. This website contains some illuminating animations. (Last viewed on January 28, 2014).
[2]A. J. Berkhout, "A holographic approach to acoustic control," J. Audio Eng. Soc. **36**(12), 977–995 (1988).
[3]A. J. Berkhout, D. de Vries, and P. Vogel, "Acoustic control by wave field synthesis," J. Acoust. Soc. Am. **93**(5), 2764–2778 (1993).
[4]E. G. Williams, J. D. Maynard, and E. Skudrzyk, "Sound source reconstructions using a microphone array," J. Acoust. Soc. Am. **68**(1), 340–344 (1980).
[5]E. G. Williams, *Fourier Acoustics* (Academic Press, London, 1999), pp. 33–34.
[6]J. de Rosny and M. Fink, "Overcoming the diffraction limit in wave physics using a time-reversal mirror and a novel acoustic sink," Phys. Rev. Lett. **89**, 124301 (2002).
[7]B. E. Anderson, M. Griffa, C. Larmer, A. J. Ultrich, and P. A. Johnson "Timing reversal," Acoustics Today **4**(1), 5–15 (2008).
[8]S. G. Conti, P. Roux, and W. A. Kuperman, "Near-field time–reversal amplification," J. Acoust. Soc. Am. **121**(6), 3602–3606 (2007).
[9]J. Rosny and M. Fink, "Focusing properties of near-field time reversal," Phys. Rev. A **76**(6), 065801 (2007).
[10]T. J. Mellow, "On the sound field of a resilient disk in free space," J. Acoust. Soc. Am. **123**(4), 1880–1891 (2008).
[11]P. M. Morse and K. U. Ingard, *Theoretical Acoustics* (McGraw-Hill, New York, 1968), pp. 319–321.
[12]L. L. Beranek and T. J. Mellow, *Acoustics: Sound Fields and Transducers* (Academic Press, Oxford, 2012), pp. 536–541.
[13]I. S. Gradshteyn and I. M. Ryzhik, *Table of Integrals, Series, and Products*, 6th ed., edited by A. Jeffrey (Academic, New York, 2000), p. 930, Eq. (8.533); p. 963, Eq. (8.794.1); p. 959, Eq. (8.756.1); p. 887, Eq. (8.334.2); p. 782, Eq. (7.112.1); p. 968, Eq. (8.828.1).
[14]J. F. Kelly and R. J. McGough, "An annular superposition integral for axisymmetric radiators," J. Acoust. Soc. Am. **121**(2), 759–765 (2007).
[15]H. Backhaus and F. Trendelenburg, "Über die Richtwirkung von Kolbenmembranen (On the directivity of piston membranes)," Ztschr. f. techn. Phys. **7**, 630–635 (1927).
[16]P. J. Walker, "New developments in electrostatic loudspeakers," J. Audio Eng. Soc. **28**(11), 795–799 (1980).
[17]T. Sugimoto and Y. Nakajima, "Acoustic characteristics of a flexible sound generator based on thermoacoustic effect," J. Acoust. Soc. Am. **133**, 3231 (2013).
[18]T. Sugimoto, A. Ando, K. Ono, Y. Morita, K. Hosoda, D. Ishii, and K. Nakamura, "A lightweight push-pull acoustic transducer composed of a pair of dielectric elastomer films," J. Acoust. Soc. Am. **134**(5), EL432–EL437 (2013).
[19]Symbolic computation by Mathematica®.
[20]M. Abramowitz and I. A. Stegun, *Handbook of Mathematical Functions* (Dover, New York, 1964), p. 390, Eq. (9.1.16).